Quantitative Genetic Variation in, and Environmental Effects on, Pathogen Resistance and Temperature-Dependent Disease Severity in a Wild Trout

Paul Vincent Debes,[1,2,*] Riho Gross,[3] and Anti Vasemägi[1,3]

1. Department of Biology, University of Turku, Natura-building, 20014 Turku, Finland; 2. Department of Biosciences, University of Helsinki, Biocenter 1, Viikinkaari 9, 00790 Helsinki, Finland; 3. Department of Aquaculture, Estonian University of Life Sciences, 48 Kreutzwaldi Street, 51006 Tartu, Estonia

Submitted June 14, 2016; Accepted March 21, 2017; Electronically published June 23, 2017

Online enhancements: appendix. *Dryad data:* http://dx.doi.org/10.5061/dryad.12758.

ABSTRACT: Health after pathogen contact varies among individuals because of differences in pathogen load (which is limited by resistance) and disease severity in response to pathogen load (which is limited by tolerance). To understand pathogen-induced host evolution, it is critical to know not only the relative contributions of nongenetic and genetic variation to resistance and tolerance but also how they change environmentally. We quantified nongenetic and genetic variation in parasite load and the associated temperature-dependent disease among trout siblings from two rivers. We detected a genetic variance for parasite load 6.6 times as large in the colder river. By contrast, genetic variance for disease traits tended to be larger in the warmer river, where the disease was manifested more severely. The relationships between disease severity and pathogen load (tolerance) exhibited plateaus at low pathogen load and stronger steepening slopes at high pathogen load in the warmer river. Our study demonstrates the environmental influence on disease severity, nongenetic and genetic variance for health-damage-limiting host abilities, and the shape of tolerance curves. Environmental variability is predicted to govern the presence and intensity of selection, change the relative contributions of nongenetic and genetic variance, and therefore hamper evolution toward more resistant and tolerant hosts.

Keywords: resistance, tolerance, heritability, genetic correlation, proliferative kidney disease, animal mixed model.

Introduction

An important but often unrecognized factor in understanding pathogen-induced host evolution is the environment (Scholthof 2007; Martin et al. 2011; Vander Wal et al. 2014; Seppälä 2015). The environment not only modifies many diseases (Walker 1965; Scholthof 2007) but also may alter the relative contributions of environment and genetics to many phenotypic traits (reviewed by Hoffmann and Merilä 1999; Charmantier and Garant 2005), the selection strength acting on them (Wilson et al. 2006), or both simultaneously (Rausher 1992; Kruuk et al. 2008). However, how the environment modifies the relative contributions of environmental and genetic effects underlying pathological phenotypes and how it may affect pathogen-driven host evolution remain largely unknown (Baucom and de Roode 2011; Martin et al. 2011; Seppälä 2015). This paucity of information is exacerbated by limited studies of environmental and genetic correlations between traits that may either restrain or facilitate the evolution of pathological phenotypes. For example, unrecognized environmental correlations between traits, or between traits and fitness, can inflate genetic-variation or selection-strength estimates and cause misleading predictions about whether and how evolution can act (Rausher 1992; Kruuk et al. 2003, 2008; Morrissey et al. 2010).

During the past decade, the potential for pathogen-induced host evolution in natural animal populations has been investigated by quantifying genetic variance for abilities that limit pathogen-induced health damage. In particular, abilities have been investigated that limit pathogen load (i.e., resistance) or limit health damage in relation to pathogen load (Lefèvre et al. 2011; Vale and Little 2012; Hayward et al. 2014*a*, 2014*b*; Mazé-Guilmo et al. 2014). The latter has been further divided into limiting health damage at a given pathogen load ("point tolerance") and limiting the health-damage increase with pathogen-load increase (i.e., the reaction-norm or dose-response curve, "tolerance"; Råberg et al. 2007; Baucom and de Roode 2011; Ayres and Schneider 2012; Medzhitov et al. 2012; Råberg 2014; Louie

* Corresponding author; e-mail: paul.debes@dal.ca.

Am. Nat. 2017. Vol. 190, pp. 244–265.
DOI: 10.1086/692536

et al. 2016). The abilities limiting either pathogen load or health damage are expected, for simple pathogen-host systems, to have different effects on host evolution and pathogen-host coevolution (Rosenthal and Kotanen 1994; Fineblum and Rausher 1995; Roy and Kirchner 2000; Restif and Koella 2004; Best et al. 2008; Boots et al. 2012). Nonetheless, as suggested for plants but largely unexplored in animals (Seppälä 2015), the relative contribution of either of these abilities to fitness and the concomitant trade-offs are expected to vary with the health-damage extent determined by the nongenetic environment (Stowe et al. 2000; Weis et al. 2000). Understanding nongenetic and genetic contributions to pathogen resistance and disease tolerance, and how the environment can modify their relative contributions, is of wide-reaching interest to medical, agricultural, and ecological and evolutionary biological research. For example, we can make valid evolutionary predictions only if we understand the environmental dependencies that regulate the relative importance of nongenetic and genetic variation (Charmantier and Garant 2005), and this premise extends to variation of abilities limiting pathogen-induced health damage (Wolinska and King 2009; Baucom and de Roode 2011; Lively et al. 2014; Vander Wal et al. 2014).

Here, we study variation in resistance to a myxozoan parasite (*Tetracapsuloides bryosalmonae*) and tolerance to the temperature-dependent disease it causes (proliferative kidney disease [PKD]) between fish-host populations (brown trout; *Salmo trutta*) from two neighboring rivers with different water temperatures. We quantified relative pathogen load (RPL) and health damage across RPL among 664 full- and half-sibling young-of-the-year fish. The resemblance among siblings, in combination with our sampling design, allowed us to decompose total phenotypic variance (σ^2_P) for RPL and health damage across RPL into additive genetic (σ^2_a), environmental spatial within-river (σ^2_{Area}), and environmental residual (σ^2_R) components. We quantified health damage according to the severity of three traits: kidney enlargement, which reflects parasite-induced kidney-tissue damage; hematocrit, which reflects parasite-induced anemia; and length-controlled epaxial muscle depth, which reflects body condition and thus disease-associated mass loss. To also assess evolutionary constraints among traits, we partitioned the phenotypic correlations (r_P) between the disease traits across RPL into environmental and genetic components. Between rivers, we discovered pronounced differences for both genetic resistance variance and overall tolerance slopes; we also discovered trends for differences in phenotypic correlations of disease-severity traits. Because water temperature is the major environmental determinant of disease severity and individuals from the two rivers showed only weak differences based on neutral genetic markers, we discuss between-rivers differences largely with respect to water-temperature differences. Our results not only exemplify how nongenetic and genetic contributions to resistance and health damage across RPL vary environmentally but also contribute to our understanding of how environmental variability may hamper pathogen-induced host evolution in nature.

Methods

Study System

PKD is a parasite-triggered and environmentally governed disease that occurs in salmonid fishes throughout the Northern Hemisphere (reviewed by Okamura et al. 2011). *Tetracapsuloides bryosalmonae*, the microscopic endoparasite that can cause PKD, has a complex life cycle with two hosts, freshwater bryozoans and salmonids; each host is infected by a different parasite stage. Fish-host infection, PKD-associated health damage, and eventually mortality critically depend on temperature. Fish are infected by waterborne *T. bryosalmonae* actinospores (Longshaw et al. 2002), which develop in sedentary freshwater bryozoans. Bryozoans become infected either by vertical transmission from their colonial parents (Hill and Okamura 2007) or by waterborne *T. bryosalmonae* myxospores, which develop in infected fish (Anderson et al. 1999; Morris and Adams 2006). Thus, direct same-species coinfection dynamics, suggested to be important for pathogen virulence evolution (e.g., Mackinnon and Read 1999), host defense mechanisms (Roy and Kirchner 2000; Boots et al. 2012), or behavioral tolerance (Adelman and Hawley 2017), appear to be less important for the hosts. Bryozoans release masses of actinospores in spring to early summer at water temperatures above 14°C (Clifton-Hadley et al. 1986; Gay et al. 2001; Tops et al. 2006). The mass release of actinospores likely results in synchronized fish infections, occurring as rapidly as 1 min and reaching 100% prevalence within 10 min (Longshaw et al. 2002). Once attached, amoeboid parasite stages leave the actinospore and enter the fish via the skin or gills, propagating in the blood until they reach the kidney. In the kidney, proliferation occurs, producing histozoic (within kidney tissue) and later also coelozoic stages (within kidney tubules). The histozoic stages are extrasporogonic (i.e., they do not produce myxospores), multiply, and can induce considerable kidney tissue damage and enlargement (Clifton-Hadley et al. 1987; Bettge et al. 2009). The coelozoic stages are sporogonic (i.e., they produce the myxospores that infect the bryozoan hosts; reviewed by Okamura et al. 2011). A time lag of 6–8 weeks may be present between infection of a fish and production of myxospores, which are excreted via urine (Kumar et al. 2013). Fish remain infective to bryozoans for at least 2 years (Abd-Elfattah et al. 2014), but longer periods appear not to have been investigated yet.

PKD-associated fish-host health damage can be quantified by several traits. The presence of the histozoic parasite in kidney tissue produces renal hyperplasia (Clifton-Hadley

et al. 1987; Bettge et al. 2009) concomitant with impaired kidney function (Hedrick et al. 1993). Importantly, the extent of kidney enlargement increases with water temperature, whereas the parasite propagation rate appears largely stable (Bettge et al. 2009); that is, disease severity (underlying parasite virulence, host immunopathology, or both) increases with water temperature. Likely as result of altered kidney tissue (the hematopoietic tissue in fishes), the hematocrit decreases; that is, anemia emerges (Hedrick et al. 1993). Anemia has been considered the most severe health consequence of PKD (Hedrick et al. 1993). Anemia decreases fish performance by lowering active metabolic rate, aerobic scope, and upper thermal tolerance (Bruneaux et al. 2017). The PKD mortality rates can be 95%–100% in captivity (Hedrick et al. 1993) and increase with water temperature (Bettge et al. 2009) but are largely unknown for wild fish (Okamura et al. 2011), although 85% mortality was estimated for wild Atlantic salmon (*Salmo salar*; Sterud et al. 2007). Infected wild fish usually exhibit pathological PKD as young of the year, and if the fish survives, the disease ceases after 14–25 weeks, usually when temperature decreases in autumn (Hedrick et al. 1993; Schmidt-Posthaus et al. 2012; Kumar et al. 2013). Immunity to the disease is acquired; that is, wild fish do not get PKD repeatedly at older ages, even though they can be reinfected with the parasite (Ferguson 1981; Okamura et al. 2011). Altogether, this parasite-host system is ideal for studying the variation of pathological phenotypes in nature because the large challenges associated with field data, such as differences in host age, infection onset, and conspecific coinfection dynamics (Bishop et al. 2012; Doeschl-Wilson et al. 2012) or host exposure avoidance (Graham et al. 2011) are minimized or absent.

Rivers, Field Sampling, Hematocrit

The two coastal Estonian rivers sampled in this study (Altja and Mustoja Rivers; fig. 1) harbor anadromous *Salmo trutta* ("sea trout") that undertake common feeding migrations in the nearby Baltic Sea. During several years of our own electrofishing and the yearly governmental salmonid survey (M. Kesler, personal communication), it has been observed that both rivers hold juveniles and small males throughout the year but no large adults, which enter the rivers only for spawning between late summer and autumn. Both rivers are relatively small, several meters wide and mostly less than 1 m deep; both are anthropogenically dammed some kilometers upstream from the sampling sites, which prevents access to upstream areas. Several beaver dams in the smaller Altja, one directly downstream from the sampled area I (fig. 1), may temporally create barriers for returning spawners. Together, this setting likely results in high gene flow between rivers, as indicated by low genetic differentiation inferred by a previous study (Gross et al. 2013) and our study ($F_{ST} = 0.004$, based on full-sib pruned data, or $F_{ST} = 0.010$, based on all offspring data; "Assessment of Population Structure" in the appendix, available online).

Between May 31 and September 22, 2014, we recorded water temperature daily at noon and midnight at sampling sites, using loggers (HOBO 8K Pendant Temperature/Alarm Data Logger, Onset Computer, Bourne, MA). Between September 19 and 24, 2014, we sampled 680 young-of-the-year trout (identified by size, 49.5–102 mm; Altja: $n = 323$; Mustoja: $n = 357$), alternating daily between rivers. We electrofished four consecutive areas per river (fig. 1*B*, 1*C*) with, depending on catch rate, three to five batches per area. We

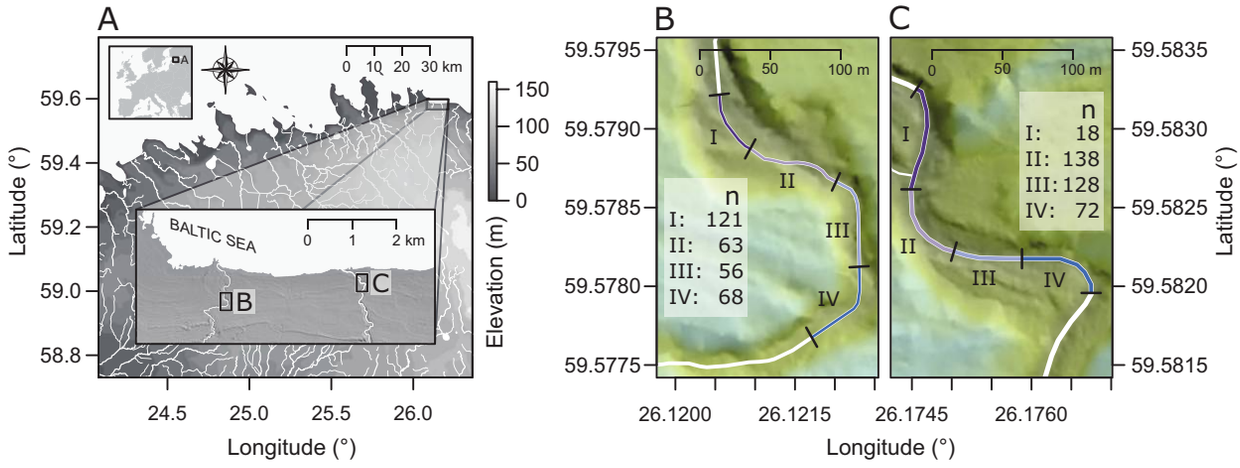

Figure 1: Location of the two sampled Estonian rivers (*A*) and the four sampled areas within the Altja River (*B*) and the Mustoja River (*C*). In *B* and *C*, the number of analyzed individuals (*n*) from each area is indicated. Areas are designated by Roman numerals and differentiated by color.

caught 5–82 individuals per batch, euthanized individuals separately by anesthetic overdose (buffered MS-222, Sigma-Aldrich, St. Louis), and measured body size (fork length ± 1 mm). We sampled blood by tail ablation with heparinized capillaries (0.5–0.6-mm diameter; Marienfeld, Lauda-Königshofen, Germany) that we immediately centrifuged at 12,250 *g* for 5 min (Haematocrit 24, Hettich, Tuttlingen, Germany). We defined the hematocrit as the red blood cell–to–total volume ratio, determined with a ruler (±0.5 mm). Next, we cut each individual dorsoventrally anterior and posterior to the dorsal fin. To determine both kidney and muscle depth (see below), we laid each resulting cross section with the anterior side upward on scale paper and took digital photographs with standardized settings (angle, distance, etc.). We preserved the cross sections for DNA extraction by freezing them in liquid N_2 and storing them at −80°C.

To estimate the relationships between traits and body size for uninfected individuals, we performed a less extensive sampling on September 26 and 28, 2015, in three parasite-negative Estonian rivers (Preedi, Treppoja, and Vodja; Dash and Vasemägi 2014) with 8–20 individuals per river, totaling 37.

Kidney and Muscle Depth

Using ImageJ 1.46r (Schneider et al. 2012), we measured the distance between the lower and upper kidney boundaries (kidney depth; in pixels) and between the upper kidney boundary and the root of the dorsal fin (muscle depth) along the sagittal cross-section plane, as depicted in Bruneaux et al. (2017). In addition, we measured a 30-mm distance per picture to transform pixels to millimeters. For uninfected individuals, kidney and muscle depth relate linearly to body size ("Traits in Uninfected Individuals" in the appendix), enabling size standardization for the focal traits by regressing them against mean centered size. When size is standardized, the traits quantify kidney enlargement (kidney depth) and body condition (muscle depth). We used a muscle-depth-based condition index because it is, unlike mass-based indexes, unaffected by ingestion state or disease-associated kidney enlargement and body-fluid disequilibrium.

DNA Extraction, Microsatellites, Kin Relationship

We estimated σ_a^2 on the basis of resemblances among relatives, using animal mixed models (see below) that require knowledge about relatedness. Because of a polygamous mating system with hundreds of offspring, the brown trout is ideal for quantifying genetic variation in nature among relatives, with many maternal and paternal full and half siblings. We inferred relatedness by using parental reconstruction based on 14 microsatellites. To do so and to provide DNA for the quantitative polymerase chain reaction (qPCR; see below), we extracted DNA from kidney tissue of each sample according to Aljanabi and Martinez (1997), assessed DNA concentration and purity photospectrometrically (ND-1000, Thermo Fisher Scientific, Wilmington, DE) with a quality criterion of the absorption ratio (260 : 280 nm) of approximately 2, and adjusted the concentrations to 10–100 ng $*$ μL^{-1} with double-distilled H_2O. Initially, we electrophoresed all samples by multiplex PCR for 15 microsatellites ("Microsatellite Loci and Multiplex PCR" in the appendix; we discarded one locus), using an Applied Biosystems 3130*xl* Genetic Analyzer (Thermo Fisher Scientific), and manually inspected and scored the genotypes, using GeneMarker (SoftGenetics, State College, PA). We amplified and genotyped 117 randomly selected samples (17%) twice to estimate error rates for allelic dropout and falsely scored alleles, using maximum likelihood as implemented in PEDANT 1.0 (Johnson and Haydon 2007). These errors provided weights in the parental reconstruction per river, based on maximum likelihood, for genotypes with at least 10 loci scored (averaging 13.9 of 14 loci; 7 samples failed), which used COLONY 2.0.5.8 (Jones and Wang 2010). As settings, we used polygamy and a weak sibship prior of 2 for both sexes, ongoing updates of parental allele-frequency estimates, long runs, and a high likelihood precision. The average likelihoods of the reconstructed pedigrees were 0.52 (Altja) and 0.70 (Mustoja). Reliable reconstruction was also indicated by a high similarity between pedigrees for a subset of 255 Altja individuals, based on either the 14 microsatellites or 1,728 single-nucleotide polymorphisms (215 out of 220 full-sib ties were equal; F. Ahmad, P. V. Debes, G. Palomar, and A. Vasemägi, unpublished manuscript).

Determination of Relative Parasite Load

Quantitative PCR (qPCR) Assay. We determined RPL in kidney tissue by qPCR. We quantified a conserved 166-bp *T. bryosalmonae* 18S ribosomal DNA fragment (TB; GenBank accession U70623) relative to a 74-bp *S. trutta* nuclear fragment (ST; putative prefoldin subunit 6; GenBank accession BT049744.1). Quantifying both genes allows the parasite DNA to be standardized to the amount of trout DNA in the assay, providing RPL. The primers used have previously been described (ST: Bruneaux et al. 2017; TB: Grabner and El-Matbouli 2009). The ST gene is a single-copy gene, whereas the TB gene is a multicopy gene that increases the assay sensitivity for the microscopic parasite. It is unknown whether TB gene copies vary among parasites, which would make the assay unreliable (Horn et al. 2010). However, previous research indicates that this assay is reliable because, first, qPCR-determined parasite copy number increases with disease progression and, second, qPCR results correlated with immunohistochemical examination results for intermediate parasite numbers (Bettge et al. 2009). The qPCR method has even been suggested to be superior to the immunohistochemical method at low and high parasite numbers, at which

the latter method suffers from spatial heterogeneity and saturation effects, respectively (Bettge et al. 2009). Moreover, parasite copy-number variants would be detected as environmental variation, not as genetic host variation, by our mixed-model analysis (see below).

In total, we ran 83 plates (96-well plates; MicroAmp Fast Optical, Thermo Fisher Scientific) on an Applied Biosystems 7500 Fast Real-Time PCR System (Thermo Fisher Scientific). Each 20-μL reaction contained 200 nM of each primer, 1 × HOT FIREPol EvaGreen qPCR Mix Plus ROX master mix (Solis BioDyne, Tartu, Estonia), and 2 μL template DNA (10–100 ng $*$ μL^{-1}). To minimize contamination, we used a laminar-flow clean bench that we UV-treated between preparations. The following amplification protocol was performed: 15 min at 95°C and 40 cycles of 15 s at 95°C, 15 s at 61°C, and 40 s at 72°C, followed by a dissociation-curve analysis between 60° and 95°C to verify amplification specificity. Each sample was run on one to four plates with triplicates per gene and plate. All plates included three no-template controls per gene to detect contamination (none detected).

Generally, qPCR assays exhibit technical bias among runs and genes in amplification efficiency (E) and quantification cycle (C_q; Pfaffl 2001), which may heavily blur quantitative genetic parameter estimates if uncorrected. To enable standardization in both E and C_q, we included a reference sample (a DNA mix of four individuals) on all plates. This reference was included as a four-point $\log_{10}$ dilution between 0.1 and 100 ng $*$ μL^{-1}, each in triplicate, on all plates. To minimize technical handling bias, we prepared all dilutions simultaneously, premixed primers, stored dilutions and primers as daily aliquots at −20°C in low-adsorption tubes (DNA LoBind, Eppendorf, Köln, Germany), and thawed each tube only once. The average E values based on dilution slopes ($E = 10^{-1/\text{slope}}$) were 1.896 ± 0.005 (TB) and 1.914 ± 0.007 (ST) ("Quantitative PCR Assay and Data Processing" in the appendix). For samples whose C_q exceeded the dilution-series range (TB C_q is unpredictable before qPCR), we repeated the assay with a template concentration that ensured that the C_q fell within the known linear assay range.

Quantitative PCR Data Processing. We applied a stringent quality-control and statistical method to account for technical bias in E and C_q among both plates and wells, enabled by assay design, high replication, and the presence of dilution series on each plate. A detailed description of the statistical procedures that enabled us to estimate technical-bias-minimized RPL for each individual can be found in "Quantitative PCR Assay and Data Processing," in the appendix.

Analysis of Water Temperature

To assess differences in water-temperature regimes between the rivers, we tested for differences in mean at the average date, temporal trends, and diurnal fluctuations based on a time-series model for the temperature records. The linear mixed model (LMM) contained fixed effects for rivers (River), second-order orthogonal date polynomials (Date.cont), factorial diurnal-fluctuation midnight and noon effects (Time), and interactions of river with both date and diurnal-fluctuation effects. We fitted factorial random date effects (*Date.fac*; random terms, here and elsewhere, are in italics) with a temporal autocorrelation of order 1 (AR(1); proportionality constant $r = 0.832 \pm 0.025$; likelihood ratio test [LRT]; $\chi^2_1 = 1{,}859.06$, $P < .001$) and random date-by-diurnal-fluctuation effects to model common trend deviations ($\chi^2_1 = 48.30$, $P < .001$). We also modeled residuals with an AR(1) date correlation ($r = 0.743 \pm 0.036$; $\chi^2_1 = 194.45$, $P < .001$). We specified the model as

$$\begin{aligned} y = {} & \text{River} + \text{Time} + \text{Date.cont} + \text{Date.cont}^2 \\ & + (\text{River} \times \text{Time}) + (\text{River} \times \text{Date.cont}) \\ & + (\text{River} \times \text{Date.cont}^2) + \textit{Date.fac} \\ & + (\textit{Date.fac} \times \textit{Time}) + \textit{Residual}. \end{aligned} \tag{1}$$

Analysis of Pathogen Load and Health Damage across Pathogen Load

Both the RPL data (see "Results") and the model residuals (not shown) were negatively skewed. Such skewness may be present for many reasons, such as spatial within-river parasite exposure heterogeneity or a mixture of distributions for abilities in limiting parasite infection and limiting parasite propagation; both contribute to the here-quantified overall resistance. On the basis of our analysis, we could exclude the former possibility because of the presence of nonsignificant area effects that would detect such a spatial nongenetic effect (see "Results"). To fulfil LMM normality assumptions and make the regression parameters of the polynomial regression (for which RPL served as a covariate; see below) biologically more meaningful (Morrissey and Liefting 2016), we used a power transformation to remove the skew: $y^\lambda = (y^\lambda - 1)/\lambda$ ($\lambda = 2.2935$; "Determining λ for an RPL Transformation" in the appendix).

For transformed RPL (variance scaled and mean centered), we estimated nongenetic and genetic variation, using an animal LMM (reviewed by Wilson et al. 2010). An animal LMM estimates σ^2_a on the basis of the expected additive genetic correlation among individuals through the inverse of the additive numerator-relationship matrix ($\mathbf{A}^{-1}$; Henderson 1973). The matrix includes the coefficients of relationship, that is, the theoretical probabilities by which pairs of individuals share common alleles, which differ between full sibs, half sibs, cousins, and so on. In contrast to family, sire, or sire-dam LMMs, which require several calculation steps to extract nongenetic and genetic variance components, animal LMMs allow them to be estimated directly.

Importantly, animal models enable nonconstant genetic variance to be modeled across a covariate at only the genetic level, whereas a family or sire model also requires the modeling of nonconstant genetic variance at the residual level, where nonconstant genetic variance is confounded with nonconstant residual variance (Lillehammer et al. 2009). Furthermore, variance estimates by animal LMMs also hold in the presence of—among other advantages—unequal sample sizes either for the different relationships with different, or even partly unknown, coefficients of relationship or for the environmental conditions, which are often variable in studies of natural systems (reviewed by Kruuk 2004). The animal model is therefore ideal for estimating σ^2_a for the herein-studied wild, polygamous host fish with many offspring per parent. We calculated $\mathbf{A}^{-1}$ on the basis of microsatellite-derived pedigree and using the asreml.Ainverse function of the ASReml-R package (Butler et al. 2009).

We specified the full LMM as

$$y = \text{River} + \text{Size} + (\text{River} \times \text{Size}) + \textit{Area} + \textit{Animal} + (\textit{Area} \times \textit{Size}) + \textit{Residual}, \quad (2)$$

with fixed terms for the two rivers (River), to test and account for differences between rivers; continuous body-size effects (Size; mean centered and variance scaled), to control for size; and the interaction of river with size (River × Size) and random terms for both additive genetic animal (*Animal*) and residual (*Residual*) effects, estimating σ^2_a and σ^2_R, respectively (σ^2_R combines random environmental and potential nonadditive genetic effects). We allowed both σ^2_a and σ^2_R to differ between rivers. Our sampling design was accounted for by additional random terms for spatial nongenetic intercept variance among the areas within rivers (*Area*; estimating $\sigma^2_{\text{Area(I)}}$) and the interaction of areas with size, that is, slopes (*Area* × *Size*; estimating $\sigma^2_{\text{Area(S)}}$). The area terms capture all spatially heterogeneous, nongenetic within-river effects with respect to the fish host, such as potential spatial heterogeneities of either parasite strains with different virulence or different parasite abundances. If unaccounted for, spatially heterogeneous environmental effects can inflate σ^2_a estimates (Henderson 1973; Kruuk and Hadfield 2007).

Because we detected an association between RPL and body size (see "Results"), we also tested for genetic (ρ_a) and residual (ρ_R) correlations between them. First, we selected a univariate LMM for body size similar to equation (2) (without the size covariate) and then specified a bivariate LMM for the responses of size and RPL, with predictors chosen on the basis of the univariate models (but without the size covariate for RPL), and fitted between-traits covariance for genetic and residual effects (area effects were not detected; see "Results").

We also assessed whether the estimated pedigrees resulted in different bias or precision for the RPL σ^2_a estimates that underlie pedigree-structure differences between rivers (e.g., number of parents, family sizes, confounding of genetic with spatial effects). To do so, we parametrically simulated 10,000 data sets based on the fixed coefficients and variance estimates of the RPL model but simulated σ^2_a as equal for rivers to make estimates comparable (based on the Altja estimate; "Parametric Simulations" in the appendix).

For each disease trait, we estimated nongenetic and genetic variance for health damage across RPL and assessed whether and how the variance changed across RPL by an LMM similar to equation (2). Thus, we additionally included RPL (transformed as above) as a covariate, up to second-order orthogonal polynomials (third-order polynomials were nonsignificant), that we interacted with the fixed River and the random *Area* and *Animal* terms (up to first-order polynomials for random terms). We specified LMMs, with terms as for equation (2), as follows:

$$\begin{aligned} y = {} & \text{River} + \text{Size} + (\text{River} \times \text{Size}) + \text{RPL} + \text{RPL}^2 \\ & + (\text{River} \times \text{RPL}) + (\text{River} \times \text{RPL}^2) + \textit{Area} \\ & + \textit{Animal} + (\textit{Area} \times \textit{RPL}) + (\textit{Animal} \times \textit{RPL}) \\ & + \textit{Residual}. \end{aligned} \quad (3)$$

The *Area* × *RPL* and *Animal* × *RPL* terms estimate the variance accounted for by the respective slope effects. Variance based on random slopes can indicate the presence of effect reranking across the covariate (e.g., offspring from one parent may perform better or worse relative to offspring from another parent, according to the RPL they are assessed at) and/or the presence of nonconstant variance across the covariate (e.g., the amount of genetic variance may depend on the RPL value at which it is assessed). Here, the variance estimated on the basis of *Area* × *RPL* effects corresponds to nongenetic, spatial tolerance variance among the eight areas ($S_{\text{Area(I,S)}}$, $S^2_{\text{Area(S)}}$). The variance estimated on the basis of *Animal* × *RPL* effects estimates genetic tolerance variance ($S_{\text{a(I,S)}}$, $S^2_{\text{a(S)}}$; Kause and Ødegård 2012; Kause et al. 2012; see also below). To avoid biasing the estimates for genetic tolerance variance, we allowed the residual variance to vary across RPL by fitting S^2_R for one to five RPL quantile categories and chose the most appropriate number. To make comparisons between traits easier and compute meaningful correlations between them with a multivariate model (see "Model Fitting"), we fitted the same number of residual variance strata to all three traits on the basis of the highest number chosen.

To test for and estimate the phenotypic correlation (r_P) among the disease traits and assess how it changes across RPL for each river, we fitted a multivariate model for the three traits based on the inferred fixed structure for the univariate models and estimated the between-traits covariance for each residual stratum. We then partitioned estimated r_P into environmental (r_R) and genetic (r_a) correlations for

each river by adding the random terms as for the univariate models. We first fitted a set of bivariate models, followed by a multivariate model, corresponding to the three univariate models, but estimated the 4 × 4 (for bivariate models) or 6 × 6 (for the multivariate model) covariance matrix between all intercept and slope terms (see "Multivariate Covariance Functions" in Meyer and Hill 1997).

It may seem counterintuitive to estimate genetic tolerance variance from cross-sectional samples with a single record per individual. However, the same principles apply that underlie the assumption that differences among either fixed or random slopes among populations, strains, or families (all with a single record per individual) reflect genetic tolerance variation (Råberg et al. 2007, 2009). The methodology we used, based on the animal model, was developed for genotype-by-environment interactions (reviewed for tolerance settings by Kause and Ødegård 2012 and more generally by Schaeffer 2004). In particular, the genotype-by-environment interaction is estimated as covariance between environments based on data among related individuals present in each environment (Falconer 1952). This "character-state approach," characterizing the genetic variance in each environment and the genetic covariance between them, can be approximated for many environments or environmental gradients by fitting variance functions, such as random regressions, which are also known as genetic reaction norms (de Jong 1995; Morrissey and Liefting 2016). Thus, in our cross-sectional study, the estimable genetic covariance among relatives that are distributed along the RPL gradient (i.e., regarding RPL as an "environmental gradient") makes it possible to test for and estimate the variance of genetic tolerance by using the animal model. However, we know of only one study that has estimated animal-model-based genetic tolerance variance (Kause et al. 2012), and the data requirements are not fully known. Therefore, we conducted simulations to determine the statistical power that results from combinations of different sample sizes for parents and offspring per parent for tolerance animal models under a balanced design. We found that under either a full-sib or full-sib-half-sib mating design, approximately 20,000 data points (100 offspring for each of 200 parents) are required to reach 80% power ("Genetic Tolerance Simulations" in the appendix). This number is much larger than the sample size of our study (and that of the majority of previous studies). Therefore, our inferences about genetic tolerance remain preliminary. However, we note that simpler models (i.e., based on families) require similar large sample sizes to make reliable inferences about genetic tolerance (Kause 2011).

Model Fitting

All models were fitted by residual maximum likelihood with ASReml-R. We first removed random terms that converged to 0 and chose the covariance structure by LRTs, except for tolerance variance terms. Because we found that our sample sizes had low power to detect genetic variance for tolerance ("Genetic Tolerance Simulations" in the appendix), we kept the corresponding terms in the models regardless of LRT outcome and regarded nonsignificant estimates as preliminary. Next, we tested for the presence of outliers, defined as studentized random effects (including residuals), with a Student's t distribution at a false discovery rate less than 0.05, and for violations from normal-distribution assumptions by using either the Shapiro-Wilk ($n < 1{,}000$) or the Lilliefors ($n > 1{,}000$) test, complemented by visually examining Q-Q plots. Then we tested fixed terms, using a backward selection strategy based on conditional F-tests with denominator degrees of freedom approximated according to Kenward and Roger (1997). We regarded fixed-effect and covariance terms as significant at $P < .05$ and positively constrained variance terms at $P < .1$. Regardless of significance, we retained the random area term in all models, where applicable, as it provides the error variance for testing the river term and minimized a possible confounding of common environmental effects (i.e., shared nongenetic effects) with genetic effects (Henderson 1973; Kruuk and Hadfield 2007). We emphasize that the area term fully absorbs the potential spatial heterogeneity of different parasite genotypes, potentially with different virulence, which altogether would be detected as spatial differences. For quantitative genetic models, we estimated 95% confidence intervals for (co)variance estimates as two times the standard error and for linear combinations and ratios of (co)variances (e.g., correlations) as two times the delta-method standard error. We report in-text results for the final models with standard errors. All data are publicly available from the Dryad Digital Repository: http://dx.doi.org/10.5061/dryad.12758 (Debes et al. 2017).

Results

Water Temperature

First, we tested for water-temperature differences between the rivers during the summer period (2014) that preceded fish sampling. The maximum observed temperatures were 23.3°C in the Mustoja and 20.3°C in the Altja (see fig. 2 for daily temperatures). On the basis of the time-series model, the Mustoja was 1.15° ± 0.11°C warmer than the Altja at the average date (July 27; $F_{1, 26.2} = 110.70$, $P < .001$). Moreover, the major seasonal trends differed between rivers (River × Date.cont^2: $F_{1, 33.7} = 18.50$, $P < .001$), and this was predicted as a temporal variation with no differences closer to spring and fall but a difference of up to 1.62° ± 0.16°C during summer. Diurnal fluctuations, however, were similar in the two rivers ($F_{1, 25.6} = 1.62$, $P = .214$) with 0.25° ± 0.11°C colder water at noon than at midnight ($F_{1, 30.7} = 4.98$, $P = .033$).

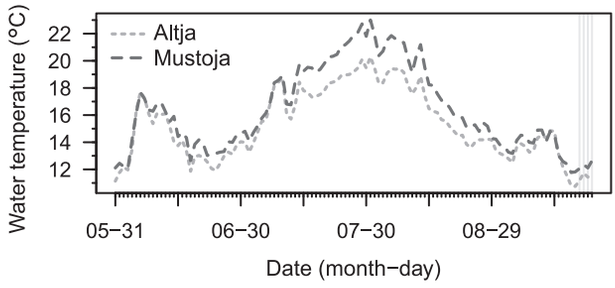

Figure 2: Average observed daily water temperatures in the two rivers during the summer of the study. Vertical light gray lines show dates when brown trout individuals were sampled.

Phenotype Data and Pedigree Structure

We obtained near-complete phenotypic and genotypic data for 308 and 356 individuals in the Altja and the Mustoja, respectively. Hematocrit data were missing for seven individuals, four in the Altja and three in the Mustoja. Using parental reconstruction, we assigned the 308 Altja offspring to 64 parents and the 356 Mustoja offspring to 124 parents. On average, we sampled 9.6 and 5.7 offspring per parent in the Altja and the Mustoja, respectively (ranges: 1–51 and 1–46, respectively). Polygamous mating was very prominent (mean partners per parent of 2.2 and 2.7 in the Altja and the Mustoja, respectively), which led to many sampled full and half sibs that delivered information about genetic variance. In both rivers, eight parents with at least 20 offspring were detected. The numbers of offspring per parent were usually distributed across several of the four areas in each river (mean areas per parent of 2.7 and 2.3 in the Altja and the Mustoja, respectively), which ensured that genetic and spatial information was not confounded ("Genetic vs. Spatial Effects" in the appendix; see also below).

Pathogen Load and Body Size

On the basis of qPCR data, we found that infection prevalence was 100%; that is, no individual exhibited complete resistance. We had quantified the inverse of resistance by relative pathogen load (RPL), which spanned a 117-fold range for the 95% percentile interval but a 1,142-fold range in total because some individuals exhibited a much lower RPL than most others (fig. 3), which motivated our power transformation. On the basis of the animal model for transformed RPL, no difference in average RPL was detected either between rivers (River: $F_{1,\,19.5} = 0.02, P = .888$, term removed) or among areas within rivers (table 1; fig. 3*C*, 3*D*); that is, we found no support for spatial environmental variation of parasite load either between or within rivers. Interestingly, we detected a negative relationship between RPL and body size ($F_{1,\,65.2} = 75.74$, $P < .001$); transformed RPL was reduced by 0.366 ± 0.041 per scaled body-size unit increase (this corresponds, after back-transformation, to halving RPL for every 18.8-mm size increase; fig. 3*A*, 3*B*). This relationship was not different between rivers (River × Size: $F_{1,\,6.5} = 0.97$, $P = .360$, term removed), nor did it vary among areas within rivers or among genotypes ($S^2_{a(S)}$ for both rivers converged to 0). Total phenotypic variance (S^2_P) for RPL was larger in the colder Altja than in the warmer Mustoja. In particular, the residual variance (S^2_R) for RPL was similar, but the additive genetic variance (S^2_a) was 6.6 times as large in the Altja (table 1; fig. 3*E*, 3*F*). The resulting heritability (h^2) was 4.4 times as large in the colder Altja as in the warmer Mustoja (h^2: 0.44 ± 0.14 in the Altja; 0.10 ± 0.09 in the Mustoja). When we removed either the (nonsignificant) spatial area term or the (significant) genetic animal terms, the variance of the removed term(s) reallocated to the residuals, indicating that spatial and genetic variances were not confounded ("Genetic vs. Spatial Effects" in the appendix). When we simulated similar genetic variance for RPL for both rivers to assess whether pedigree-quality differences resulted in S^2_a differences between rivers, river-specific estimates across 10,000 simulations were similar (simulated σ^2_a: 0.475; estimated S^2_a with 95% simulation interval: 0.457, 0.145–0.891 in the Altja and 0.463, 0.176–0.842 in the Mustoja). Relative bias and imprecision were slightly lower in the Mustoja (relative bias: 3.8% in the Altja and 2.5% in the Mustoja, imprecision: 0.75 in the Altja and 0.67 in the Mustoja).

Correlation between RPL and Body Size

We further investigated the observed negative association between RPL and body size by first selecting a univariate model for body size and then fitting a bivariate model for RPL and size, as suggested by Graham et al. (2011). On the basis of the univariate model for body size, we did not detect any spatial effects on size (S^2_{Area} converged to 0). The estimated genetic variance was remarkably similar in the two rivers (S^2_a: 0.37 ± 0.12, $\chi^2_1 = 65.82$ in the Altja and 0.35 ± 0.12, $\chi^2_1 = 25.27$ in the Mustoja; both $P < .001$). However, the average size was smaller and the size range narrower in the colder Altja than in the warmer Mustoja ($F_{1,\,77.7} = 67.15, P < .001$; fig. 3*A*, 3*B*); residual variance was nearly twice as large in the Mustoja (S^2_R: 0.214 ± 0.057 in the Altja and 0.397 ± 0.071 in the Mustoja), which, altogether, resulted in different h^2 estimates for body size between rivers (h^2: 0.628 ± 0.112 in the Altja and 0.477 ± 0.097 in the Mustoja).

For the bivariate model and when RPL was fitted without the size covariate, genetic variance estimates for RPL in both rivers were larger than those with the size covariate included (S^2_a: 0.663 ± 0.242 in the Altja and 0.157 ± 0.087 in the Mustoja). However, residual variance estimates for RPL

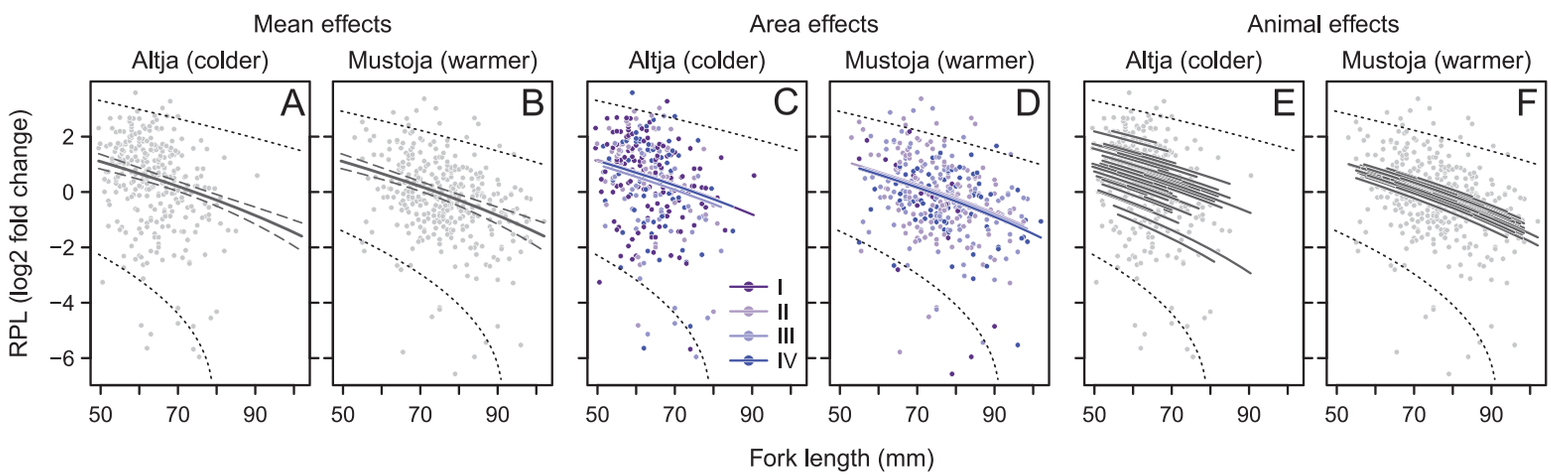

Figure 3: Model-predicted, back-transformed relationship between relative pathogen load (RPL) with *Tetracapsuloides bryosalmonae* in kidney tissue and body size of brown trout. Lower RPL indicates higher resistance. *A* and *B* show the same average relationship for both investigated rivers (Altja, Mustoja). *C* and *D* depict the (nonsignificant) spatial variation among the four investigated areas per river (fig. 1*B*, 1*C*). *E* and *F* depict the additive genetic variation, predicted as breeding values for parents with more than one offspring (55 in the Altja, 101 in the Mustoja) and plotted across the observed offspring size range (i.e., parental breeding values appear as slopes). Please note that the genetic variance represented in *E* relative to that in *F* is 6.6 times as large. Dashed lines in *A* and *B* show the 95% confidence intervals of the regression lines. Dotted lines in all panels show the 95% prediction intervals. Dots in all panels, in gray or with colors that correspond to areas in *C* and *D*, show the observed offspring data. Lines for mean effects are based on the best linear unbiased estimators, and lines for area and animal effects are based on the best linear unbiased predictors.

Table 1: Likelihood ratio test results for random terms and their residual maximum likelihood estimates for relative parasite load (RPL, resistance^{-1}), controlled for body size

River, term	χ^2_1	P	Estimate (SE)
Both:			
$\sigma^2_{\text{Area(I)}}$	.50	.480	.007 (.011)
$\sigma^2_{\text{Area(S)}}$ [a]	.28	.599	.010 (.015)
Altja:			
$\sigma^2_{\text{a(I)}}$	27.99	**<.001**	.475 (.186)
σ^2_{R}	...	...	.602 (.128)
Mustoja:			
$\sigma^2_{\text{a(I)}}$	3.13	**.077**	.072 (.060)
σ^2_{R}	...	...	.618 (.069)

Note: The terms are for spatial area (σ^2_{Area}), additive genetic (σ^2_{a}), or residual (σ^2_{R}) variance, whereby the subscripts "I" and "S" in parentheses indicate "intercept" (at average body size) and "slope" (across mean-centered body size), respectively. Slope effects were also tested for σ^2_{a} per river, but the variance estimates converged to 0. Boldface indicates significant results ($P < .1$).

[a] Random term was removed from the model.

remained similar, indicating that much of the association between RPL and size in the univariate model resulted from genetics. This was further supported by estimated correlations between RPL and size that were exclusively negative in sign and both stronger and estimated with more confidence at the genetic (r_{a}) than at the environmental residual (r_{R}) level (r_{a}: -0.44 ± 0.27 in the Altja and -0.70 ± 0.34 in the Mustoja; r_{R}: -0.13 ± 0.24 in the Altja and -0.23 ± 0.13 in the Mustoja). Of the correlations, only r_{a} in the Mustoja was strictly significant at the 5% alpha level (r_{a}: $\chi^2_1 = 3.54$, $P = .060$ in the Altja and $\chi^2_1 = 5.13$, $P = .002$ in the Mustoja; r_{R}: $\chi^2_1 = 0.26$, $P = .610$ in the Altja and $\chi^2_1 = 2.72$, $P = .099$ in the Mustoja).

Disease Severity and Tolerance

Next, we assessed health at the average parasite load and the relationship between health and parasite load ("tolerance") for each disease trait. On the basis of univariate models, we could not detect differences between rivers for any of the three disease traits at the average parasite load (table 2). Furthermore, intercepts did not differ among the areas for kidney enlargement, but they differed for hematocrit and body condition ($S^2_{\text{Area(I)}}$; table 3); that is, we found support for spatial environmental variation of health for two traits within but not between rivers. The strongest spatial effects were detected for hematocrit, whereby area I in the Altja and area III in the Mustoja (fig. 1*B*, 1*C*) housed fish with below- and above-average hematocrit values, respectively ("Area effects" in fig. 4).

The health of the trout decreased with increasing RPL. Thus, with increasing parasite load, health decreased in the form of enlarging kidney, decreasing hematocrit, and decreasing body condition (fig. 4). The relationships were nonlinear: the chosen models included second-order polynomials; either the first- or second-order polynomials or both differed between rivers (table 2). Even though polynomials prevent asymptotic relationships from being directly modeled, the modeled relationships exhibited—after the back-transformation of RPL—either a sigmoidal relationship (kidney enlargement) or plateau-like segments at low parasite load and a missed asymptotic-like segment at high RPL (hematocrit, body condition). Notably, health decline with parasite-load increase, which started after the plateau, was steeper for all three traits in the warmer Mustoja ("Mean effects" in fig. 4). In other words, average disease tolerance was significantly lower in the warmer Mustoja than in the colder Altja.

The estimated total phenotypic variance (S^2_{P}) for health tended to be larger in the warmer Mustoja than in the colder Altja for all three disease traits (1.2–1.6 times as large; table 3; fig. 4). Apart from the detected presence of spatial area variances (see above), we also detected significant additive genetic variance ($\sigma^2_{\text{a(I)}}$) for all three traits that, in contrast to what was found for resistance, tended to be larger in the warmer Mustoja (table 3; fig. 4). The evidence for $\sigma^2_{\text{a(I)}}$, judged by LRT statistics (table 3), was stronger for kidney enlargement and body condition in the warmer Mustoja than in the colder Altja but similar for hematocrit. The residual variance (S^2_{R}) differed significantly across RPL for kidney enlargement (two residual strata across RPL improved

Table 2: ANOVA for fixed terms of the chosen mixed animal model for each of the three disease traits

Trait, term	DF	DDF	F	P
Kidney depth:				
Size	1	543.1	99.78	**<.001**
River	1	23.4	.03	.876
RPL	1	322.2	158.70	**<.001**
RPL^2	1	374.2	30.76	**<.001**
River × RPL	1	238.7	18.59	**<.001**
Size × River	1	565.0	24.34	**<.001**
Hematocrit:				
Size	1	466.8	39.41	**<.001**
River	1	7.9	3.0	.122
RPL	1	48.4	219.40	**<.001**
RPL^2	1	231.8	17.91	**<.001**
River × RPL	1	70.9	4.86	**.031**
River × RPL^2	1	279.7	6.69	**.010**
Muscle depth:				
Size	1	571.8	6,894.0	**<.001**
River	1	11.8	.15	.704
RPL	1	32.2	59.05	**<.001**
RPL^2	1	186.3	8.31	**.004**
River × RPL	1	45.7	15.02	**.001**
River × RPL^2	1	271.1	4.03	**.046**

Note: Boldface indicates significant results ($P < .05$). DF = degrees of freedom; DDF = denominator degrees of freedom; RPL = relative pathogen load.

Table 3: Likelihood ratio test results for random terms and their univariate mixed-model residual maximum likelihood estimates for each of three disease traits (controlled for body size)

	Kidney size (mm)			Hematocrit			Muscle size (mm)		
River, term	χ^2_1	P	Estimate (SE)	χ^2_1	P	Estimate (SE)	χ^2_1	P	Estimate (se)
Both:									
$\sigma^2_{\text{Area(I)}}$	1.28	.258	.0021 (.0029)	42.71	**<.001**	.00035 (.00023)	5.91	**.015**	.0024 (.0021)
$\sigma_{\text{Area(I,S)}}$	2.27[a]	.132[a]	−.0050 (.0056)	4.21[a]	**.040**[a]	.00024 (.00019)	1.25[a]	.263[a]	−.0021 (.0022)
$\sigma^2_{\text{Area(S)}}$	.10[a]	.664[a]	.0079 (.0132)	.66[a]	.416[a]	.00019 (.00025)	…[a,b]	…[a,b]	.0021 (.0048)
Altja:									
$\sigma^2_{\text{a(I)}}$	6.71	**.010**	.0263 (.0174)	4.40	**.036**	.00038 (.00028)	5.41	**.020**	.0133 (.0082)
$\sigma_{\text{a(I,S)}}$	2.22[a]	.136[a]	−.0266 (.0234)	.00	.991	<.00001 (.00033)	.05	.836	−.0026 (.0100)
$\sigma^2_{\text{a(S)}}$	…[a,b]	…[a,b]	.0218 (.0401)	2.18	.140	.00063 (.00067)	.50	.478	.0155 (.0221)
σ^2_{R} (1)[c]			.9940 (.0401)			.00290 (.00059)			.0534 (.0154)
σ^2_{R} (2)[c]			.1819 (.0455)			.00182 (.00073)			.0417 (.0152)
σ^2_{R} (3)[c]			.1188 (.0243)			.00311 (.00056)			.0492 (.0110)
σ^2_{R} (4)[c]			.0983 (.0192)			.00149 (.00036)			.0541 (.0124)
Mustoja:									
$\sigma^2_{\text{a(I)}}$	17.11	**<.001**	.1290 (.0552)	4.20	**.040**	.00051 (.00034)	11.80	**.001**	.0185 (.0098)
$\sigma_{\text{a(I,S)}}$	.64[a]	.423[a]	.0544 (.0720)	1.48[a]	.224[a]	.00064 (.00072)	5.61[a]	**.018**[a]	.0315 (.0186)
$\sigma^2_{\text{a(S)}}$	…[a,b]	…[a,b]	.0193 (.1236)	…[a,b]	…[a,b]	.00053 (.00156)	…[a,b]	…[a,b]	.0350 (.0473)
σ^2_{R} (1)[c]			.2433 (.0598)			.00165 (.00038)			.0830 (.0152)
σ^2_{R} (2)[c]			.3326 (.0663)			.00238 (.00044)			.0647 (.0124)
σ^2_{R} (3)[c]			.4483 (.0937)			.00487 (.00087)			.0965 (.0191)
σ^2_{R} (4)[c]			.2903 (.0889)			.00594 (.00132)			.0881 (.0221)

Note: The terms are for spatial area (σ^2_{Area}), additive genetic (σ^2_{a}), or residual (σ^2_{R}) variance, whereby the subscripts "I" and "S" in parentheses indicate "intercept" and "slope" (across mean-centered relative parasite load), respectively. For area and genetic effects, $\sigma_{\text{(I, S)}}$ indicates the covariance between intercept and slope effects. Boldface indicates significant results ($P < .05$ for covariance terms or $P < .1$ for positively constrained variance terms).

[a] Term was removed from the model.

[b] Term converged to 0 when the intercept-slope covariance was constrained to be 0.

[c] The residual variance for each river and each trait is given for each of four relative-pathogen-load quantiles, indicated by the number in parentheses (see text for details).

the fit: $\chi^2_2 = 11.17$, $P = 0.004$) and hematocrit (four residual strata across RPL improved the fit: $X^2_6 = 41.94$, $P < .001$) but not for body condition. In the Altja, S^2_{R} was highest at intermediate RPL for kidney enlargement and decreased with RPL for hematocrit, whereas in the warmer Mustoja S^2_{R} increased with parasite load for both traits (fig. 4). We fitted all three models with four residual strata to facilitate the subsequent modeling of between-traits correlations.

Significant tolerance variance, that is, a change of variance across RPL caused by effect reranking, was not detected for spatial environmental ($S^2_{\text{Area(S)}}$) or additive genetic effects ($S^2_{\text{a(S)}}$) for any trait (table 3). However, because our simulations suggested that our sample sizes provided low power to test for $\sigma^2_{\text{a(S)}}$ ("Genetic Tolerance Simulations" in the appendix), we kept the genetic tolerance term in the model whenever the associated variance was estimable (but when model likelihood estimates became unstable, we removed them) and stress that estimates should be regarded as preliminary. A change of σ^2_{a} across RPL was stably estimable only in the Altja and only for hematocrit and body condition (table 3). The support for $\sigma^2_{\text{a(S)}}$ for body condition was extremely low, but for hematocrit it was close to a one-sided variance significance threshold of $P < .1$. Intercept and slope effects did not seem to be correlated for either trait (table 3). When we predicted the change of σ^2_{a} for hematocrit across RPL based on $S^2_{\text{a(I)}}$, $S_{\text{a(I,S)}}$, and $S^2_{\text{a(S)}}$ according to Fischer et al. (2004), we found that S^2_{a} in the Altja first decreased with increasing RPL and then increased, whereas the S^2_{a} confidence intervals increased toward both ends and rendered S^2_{a} not different from 0 at high RPL (not shown, but see fig. 4*K*). As a result of differing $S^2_{\text{a(I)}}$ and S^2_{R}, h^2 also differed between rivers. However, because of an additional nonconstancy of S^2_{R} for kidney enlargement and hematocrit across RPL (and of S^2_{a} for hematocrit in the Altja), h^2 for these traits additionally depended on RPL (specific estimates can be calculated from table 3).

Correlations between Disease Traits

Results from a multivariate model without random terms indicated that all three traits were phenotypically correlated, except for kidney enlargement with body condition in the colder Altja, where confidence intervals across RPL included 0 (fig. 5*A*, 5*D*, 5*G*). The phenotypic correlations across RPL

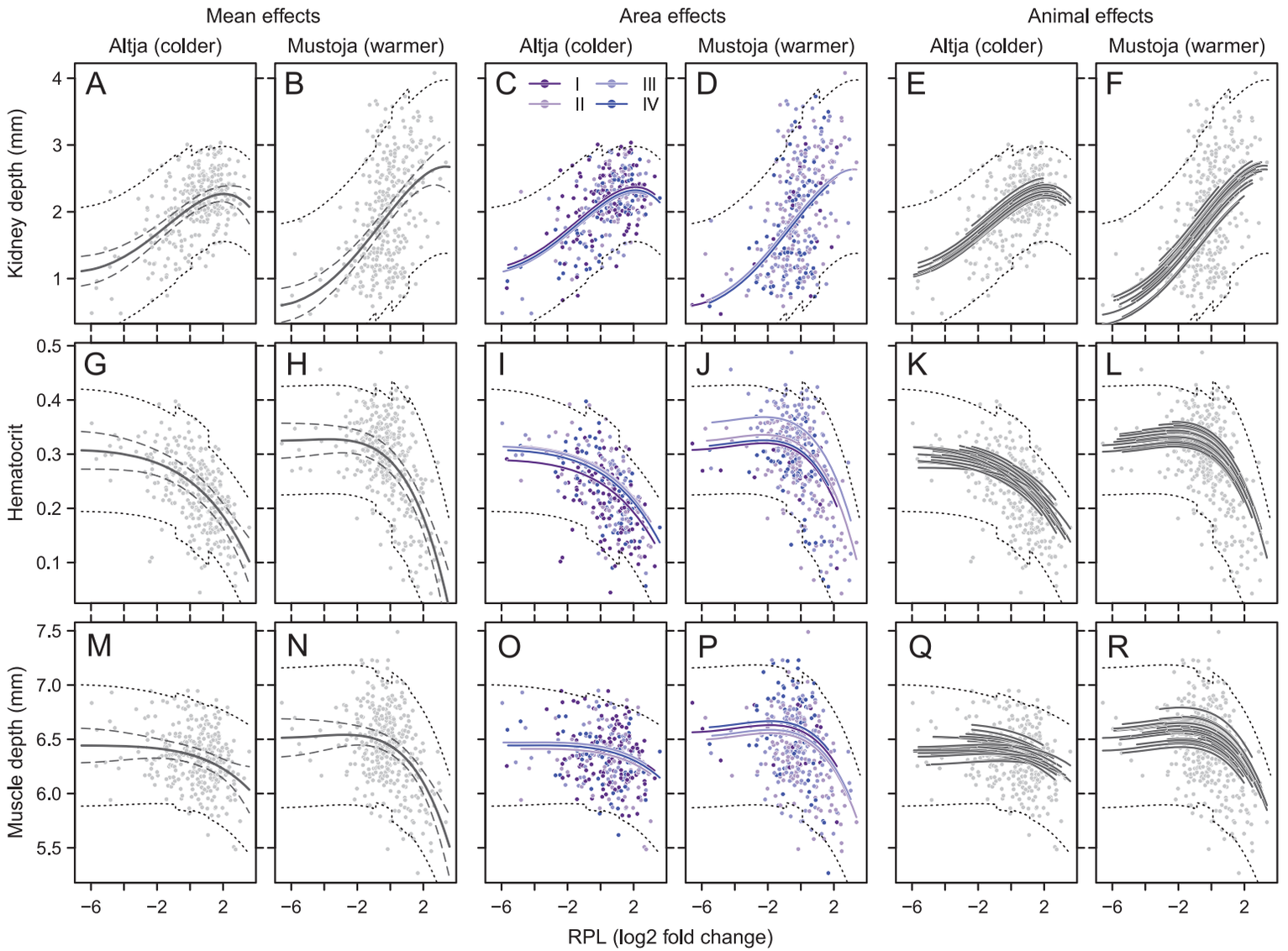

Figure 4: Model-predicted, back-transformed relationships between three disease traits and back-transformed relative *Tetracapsuloides bryosalmonae* parasite load (RPL) in brown trout kidney tissue. The first two columns show the average relationships in each river (Altja, Mustoja). The third and fourth columns depict the spatial variation among the four investigated areas per river (fig. 1*B*, 1*C*). The fifth and sixth columns depict the additive genetic variation, predicted as breeding values for parents with more than one offspring and plotted across the observed offspring RPL range. Dashed lines in the first two columns show the 95% confidence intervals of the regression lines. Dotted lines in all panels show the 95% prediction intervals. Dots in all panels, in gray or with colors that correspond to areas in the third and fourth columns, show the observed offspring phenotypes (adjusted to average size). Lines for mean effects are based on the best linear unbiased estimators, and lines for area and animal effects are based on the best linear unbiased predictors.

tended to decrease in the colder Altja and increase in the warmer Mustoja. However, judged by the extent of overlapping confidence intervals, significant differences for r_P between rivers were present only at high RPL between kidney enlargement and body condition (i.e., confidence intervals overlapped for less than half their length; fig. 5*D*). When we partitioned r_P into nongenetic and genetic correlations, using three bivariate models (a multivariate model did not converge), environmental spatial area effects did not correlate between any of the three disease traits (r_{Area}; kidney-hematocrit: $\chi^2_1 < 0.01$, $P = .974$; kidney-muscle: $\chi^2_1 = 1.32$, $P = .251$; hematocrit-muscle: $\chi^2_1 = 1.66$, $P = .197$). Nonetheless, we detected environmental between-traits correlations (r_R) for most of the four modeled residual strata in both rivers (fig. 5*B*, 5*E*, 5*H*). We obtained statistical support for the presence of genetic correlations (r_a) in the Altja between hematocrit and body condition, but not between other traits or in the Mustoja (fig. 5*C*, 5*F*, 5*I*). When we tested whether a change in genetic variance across RPL covaried between hematocrit and body condition in the Altja, that is, when we tested for genetic tolerance covariance between the two traits, we found a *P* value just greater than 5% ($\chi^2_4 = 9.22$, $P = .056$); however, the predicted correlation remained largely stable across RPL ($r_a = 0.91-0.98$; fig. 5*I*).

Discussion

We demonstrated that PKD in natural brown trout populations exhibits environmental and genetic variation for both pathogen load (which is limited by resistance) and disease severity (which is limited by resistance and tolerance). Genetically determined survival, and thus evolution under the potentially lethal disease, may therefore depend on genetic variance present for resistance and tolerance. That both resistance and tolerance can be modulated by the environment and that an environmental modulation could have considerable effects on evolutionary dynamics has often been hypothesized, but the extent and mechanisms present in natural systems have remained largely enigmatic (Martin et al. 2011; Lively et al. 2014; Seppälä 2015; Brunner and Eizaguirre 2016). The overall relationship between health and pathogen load has been termed "tolerance" or "the dose-response curve" (Råberg et al. 2007; Ayres and Schneider 2012; Louie et al. 2016). We found that tolerance to PKD differed strongly between two neighboring rivers. In particular, we found steeper tolerance slopes and stronger health damage in the warmer river (Mustoja) than in the colder river (Altja), even though the average pathogen loads were equal between rivers. Because health damage, that is, PKD severity, increases with water temperature, which may be linked to either a higher pathogen virulence or a stronger host overreaction (immunopathology; reviewed by Graham et al. 2011; Medzhitov et al. 2012), it is likely that the profound temperature differences between rivers caused the observed tolerance-curve differences. Furthermore, we detected pronounced between-rivers differences for nongenetic and genetic contributions to phenotypic variances for both resistance and disease severity across pathogen load and for phenotypic correlations between the disease traits. Our study, therefore, exemplifies the importance of environmental effects not only on tolerance-curve shape and the severity of health damage but also on the variability of nongenetic and genetic contributions to genetically based host abilities that limit health damage. We expect that such environmental effects on the relative contributions of nongenetic and genetic variance for resistance and tolerance are also present for many other pathogen-host systems.

Because water temperature varies not only spatially between river populations but usually also temporally among river cohorts within rivers, we expect a profound and, so far, rarely considered environmental effect on the evolution of resistance and tolerance (reviewed by Wolinska and King 2009; Lively et al. 2014). In particular, spatial and temporal temperature variability can be expected to govern disease severity and thus the selection intensity for all abilities that limit health damage. Across populations and generations, spatiotemporal variability may lead to occurrences of stronger positive selection (higher genetic values for both resistance and tolerance increase survival) and weaker or even negative selection (higher genetic values for both resistance and tolerance do not increase survival or may even be disadvantageous through fitness trade-offs), whereby selection intensity across pathogen load is defined by the environmentally governed tolerance curve. The presence and intensity of this environmentally governed selection may hamper evolution toward more resistant or tolerant populations.

In the following, we first iterate evolutionary theories on resistance and tolerance to further discuss how nongenetic and genetic effects may affect host evolution, and we also discuss the detected genetic correlation between resistance and body size. We then consider possible confounding effects between river temperatures and unknown variables and the sample sizes required to reliably detect nonconstant genetic variance across pathogen load (i.e., genetic tolerance variance). Finally, we provide an outlook for how future investigations may improve our understanding of why the relationship between health and pathogen load covaries nonlinearly by investigating the change in genetic (co)variance across a curve, using a more advanced quantitative genetics framework.

Constraints of Resistance and Tolerance Evolution

Resistance, the ability to limit pathogen load, is of evolutionary host importance only if it covaries with host fitness. Thus, resistance can evolve if the pathogen affects fitness, usually via

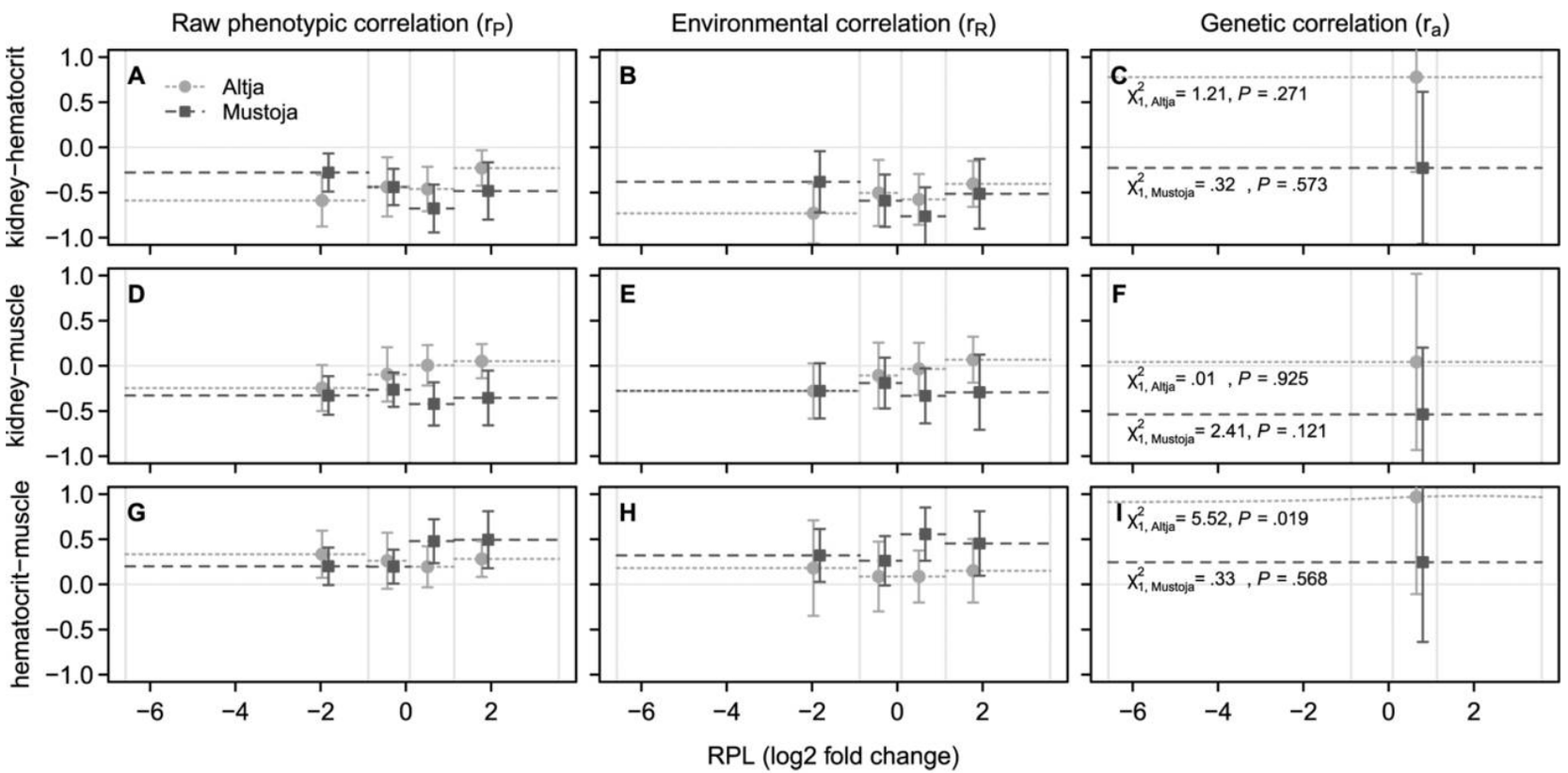

Figure 5: Estimated correlations between disease traits across relative parasite load (RPL) for the two rivers (Altja, Mustoja) based on a multivariate model (*A*, *D*, *G*) or on three bivariate models (all other panels). Phenotypic and residual (co)variances were modeled with four variance strata across RPL (variance strata borders are indicated by vertical light gray lines) that allowed four correlations to be estimated, whereas the genetic (co)variances were modeled with constant variance across RPL that allowed one correlation to be estimated. An exception is the correlation between hematocrit and muscle depth in the Altja (*I*), which was modeled with a 4 × 4 covariance matrix for intercepts and slopes that allowed the genetic (co)variances, and thus the genetic between-traits correlation, to continuously change across RPL.

expression of a disease. Tolerance, the ability to limit disease-severity increase with pathogen-load increase, can evolve if the pathogen load is sufficiently high (thus, if resistance is sufficiently low) to express a disease that is severe enough to affect fitness. According to the theory of frequency-dependent selection, selection intensity for resistance diminishes when infection probability decreases through a higher frequency of resistant individuals, which decreases the pathogen spread; eventually, resistance may be selected against by a fitness cost of being resistant (Roy and Kirchner 2000; Miller et al. 2005). By contrast, tolerance evolution may not affect infection probability among hosts and therefore lacks similar negative feedback mechanism (Roy and Kirchner 2000; Miller et al. 2005; Best et al. 2008; Boots et al. 2012). Thus, many theorists expect tolerance to be at a maximum with little within-population variation and resistance to be incomplete and highly variable. This expectation has served as an interpretation for the inability to detect genetic tolerance variance (Lefèvre et al. 2011), although testing this expectation empirically has been difficult (Hayward et al. 2014*a*). From a biological perspective, relative fitness costs arising from trade-offs for being more resistant, more tolerant, or both may also be important (Restif and Koella 2004). It remains unknown how far theories of frequency-dependent selection, predicted from models for directly transmitted (e.g., Boots and Bowers 1999; Restif and Koella 2004) or free-living (e.g., Miller et al. 2005) pathogens, can be generalized to the great diversity of host-parasite systems (reviewed by Barrett et al. 2008). In many multihost systems, such as the one presented here, indirect pathogen transmission is present. In our study system, the stage that develops in bryozoans infects fish, and the stage that develops in fish infects bryozoans. These stages are released during different seasons (Anderson et al. 1999; Morris and Adams 2006). The separation of infectious-stage production between species and seasons may limit the hypothesized frequency-dependent selection of resistance evolution by reducing the importance of epidemiological dynamics among conspecifics. Similar known temporal separations of infection onsets between multiple hosts are known for other parasites, such as the cause of whirling disease in fish, *Myxobolus cerebralis* (Neudecker et al. 2012; Sarker et al. 2015). Thus, especially in complex parasite-host systems, spatial and temporal selection intensity variation may provide an alternative explanation for why hosts remain susceptible.

Nonlinear Tolerance

We identified nonlinear tolerance relationships for all three disease traits in both rivers. Even though pathogen growth and host immune response kinetics predict curves, previous research usually identified linear relationships (Louie et al. 2016). However, only a few meaningful tolerance curves have been assessed (Ayres and Schneider 2012). In our study, the tolerance curves for all traits exhibited plateau-like parts at low pathogen load. Thus, a pathogen threshold appears necessary to induce health damage, as observed for the relationships between yield and potato-beetle damage in potatoes (*Solanum tuberosum*; Nault and Kennedy 1993) or immune-system-component expression and pathogen load in flies (Louie et al. 2016). The "real" tolerance slope, following the plateau, was steeper and led to more extreme values in the warmer river, where we expected higher disease severity because of the strong temperature dependence of the disease (Ferguson 1981; Hedrick et al. 1993; Bettge et al. 2009).

Nonlinear tolerance causes the fitness increase that results from resistance increase to be nonlinear, and this may hamper resistance evolution. Positive resistance selection occurs when an increase in resistance produces an increase in fitness, that is, only when the tolerance slope is different from 0 (when pathogen load and disease severity covary). This exact effect is absent at low pathogen loads under curves with initial plateaus (when pathogen load and disease severity do not covary). When, in addition, the steepness of the slope part of the curve varies with environmental conditions, such as here suggested by water temperature, this is expected to additionally vary selection intensity for a given pathogen load (and thus the fitness effect from increasing resistance). Temporally variable tolerance curves within rivers or spatially variable tolerance curves among rivers may therefore provide a simple mechanism for slowing down resistance evolution (reviewed by Lazzaro and Little 2009). Evolution toward resistance may be present or absent by environmental variation between conditions either favoring resistance or exposing it to genetic drift via changing both pathogen load (by a possible environmental variation in pathogen abundance) and the steepness of the tolerance slope. This environmental effect on selection presence and intensity may explain, alternatively or in addition to negative feedback mechanisms, why hosts do not reach complete resistance (Mostowy and Engelstadter 2011).

Within rivers, we detected spatial tolerance variance for hematocrit that may reflect spatial environmental quality differences (Rosenthal and Kotanen 1994). Spatial tolerance variation detected for fin damage versus ectoparasite load in a wild fish has previously been linked to variation in water temperature (Blanchet et al. 2010). Here, we are able to meaningfully associate variation of hematocrit tolerance with stream velocity. In particular, hematocrit correlates positively with active metabolic rate and aerobic scope (Bruneaux et al. 2017); that is, a high hematocrit characterizes "athletic" individuals. This relationship was reflected in the finding that hematocrit was lowest in the most stagnant area before a beaver dam in the Altja and highest in the area with stretches of shallow rapids in the Mustoja. It remains unknown, however, whether fish with low hematocrits were forced to find refuge in calm waters because of fatigue and

fish with higher hematocrits were more likely to remain in the rapids (the preferred young-of-the-year habitat) or whether hematocrits in the two areas already differed before the disease outbreak.

Strong Between-Rivers Differences in Genetic Resistance Variance and the Correlation with Size

We quantified resistance by (the inverse of) pathogen load and found that it was equal between rivers but that genetic resistance variance was 6.6 times as high in the colder river. We could exclude the possibility that a bias through pedigree differences or confounding spatial and genetic effects generated these differences. Instead, we believe that differences in genetic resistance variance may have been linked to disease-severity differences between rivers. We believe this because selection for resistance is expected via the pathological phenotype, and the differences in the relationships between the pathological phenotype and resistance are described by the differences in tolerance curves between rivers.

Nonetheless, resistance and body size exhibited a similar phenotypic correlation in the two rivers that we could attribute to mostly genetic origin, whereby size was able to explain 28% and 54% of the genetic resistance variance in the Altja and the Mustoja, respectively. A mere phenotypic correlation between resistance and size that was stable during PKD pathogenesis has been detected (Grabner and El-Matbouli 2009). Positive genetic correlations between disease resistance and size have also been observed in other fishes (summarized in Gjedrem 2005) and sheep (Coltman et al. 2001). A simple explanation for this correlation could be that both growth and resistance are positively correlated with a third trait: resource acquisition. Individuals with a high genetic value for resource acquisition may allocate overall more resources to both growth and resistance. This idea is supported by a poultry-data meta-analysis that indicates that growth selection coselects for pathogen resistance, but not vice versa, possibly as a result of fewer resources being required to enhance resistance relative to growth (van der Most et al. 2011). A positive correlation does not even contradict a theoretical resource allocation trade-off between resistance and other fitness-related traits, formulated first in plants (Simms and Rausher 1987; Rosenthal and Kotanen 1994), later adapted for animals (Sheldon and Verhulst 1996; Martin et al. 2011; Ayres and Schneider 2012), demonstrated in sheep (Hayward et al. 2014*a*), and providing a foundation for many theoretical models (e.g., Miller et al. 2005). In fact, a resource trade-off may still be present for every individual because natural selection may act on resource acquisition variability among individuals rather than on the resource trade-off within individuals (Houle 1991). Thus, resource allocation may be an indirect, evolutionarily important fitness trait for the studied disease. Both a higher resistance and a larger size are expected to increase young-of-the-year trout survival by better health under PKD (Bettge et al. 2009; Bruneaux et al. 2017) and by generally better endurance of starvation, environmental extremes, and predators (Sogard 1997). A positive correlation with resource acquisition (or size) may thus even maintain genetically based resistance in the absence of pathogen-induced selection as long as selection is positive for size, which would be of immense evolutionary importance when selection intensity varies spatially and temporally.

Many theoretical models assume that resistance is costly in the absence of the pathogen (Roy and Kirchner 2000; Miller et al. 2005). However, resistance may vary through genetic variants or be based on conditionally expressed genes (neither directly implies any extra cost under pathogen absence). Nonetheless, genetic variation for unconsidered fitness traits, such as reproductive success, may still compete with genetic variation for resistance (Graham et al. 2011). Because more resistant genotypes showed both larger size and better body condition in fall and reserves usually remain constant or are depleted during winter, we still suspect that more resistant genotypes are more likely to exhibit higher fitness.

To explain the large differences in genetic variance between rivers, it may be possible that temperature-dependent selection intensity had reduced σ_a^2 more strongly in the warmer river. This effect would require resistance to be based on relatively few loci (Bulmer 1971) and selection to be strong and much stronger in the warmer than the colder river. Resistance to whirling disease in salmonid fishes, which is caused by another aquatic myxozoan parasite with a similar life history, *M. cerebralis*, is assumed to involve one or few loci (Baerwald et al. 2011), which may explain a previously observed rapid resistance increase after *M. cerebralis* was introduced to a lake (Miller and Vincent 2008). Following this idea, average resistance (in contrast to its variance) may not have been similar between rivers before a hypothetical selection event; that is, individuals with low resistance (and a low resistance breeding value) may have died before sampling. We expected higher disease-driven severity in the warmer river because temperature-dependent health, rather than the pathogen load (which was equal between rivers), predicts PKD severity and mortality (Bettge et al. 2009), and we indeed observed more severe disease expression in the warmer river. It is therefore likely that contemporary viability selection in the study cohort (Hadfield 2008) had reduced σ_a^2 for resistance more strongly in the warmer river by removing individuals carrying detrimental alleles. Alternatively, different "resistance genes" may have been expressed in the different rivers because of different environmental conditioning, and both sets of genes may result in their own genetic variance. Such environmentally driven short-term σ_a^2 variability was suggested by Wilson et al. (2006), who found that S_a^2 for birth mass in Soay sheep

was low in years of strong selection but high in years of weak selection, which altogether was assumed to limit the evolution of birth mass (see also reviews by Hoffmann and Merilä 1999; Charmantier and Garant 2005). A similar variability for σ_a^2 for pathogen resistance may also explain the difference detected between rivers in our study, which, however, requires verification by a temporal study.

Correlations between Traits

The heritability of a pathological phenotype reflects how much of its variation among individuals underlies heritable effects (Tenesa and Haley 2013). Nonetheless, evolutionary change of the pathological phenotype is expected only if (1) it correlates with fitness not only genetically but also environmentally, (2) it is not (negatively) correlated with other traits under selection that restrain its evolution, and (3) the genetic and environmental correlations do not sum to 0 (Rausher 1992; Kruuk et al. 2003; Morrissey et al. 2010). Thus, it is of great interest to identify the magnitude and sign of genetic and environmental correlations between traits that define a disease and describe how these correlations change with either pathogen load or environmental conditions. In this study, we approximated fitness by health, which is a common practice in animal disease studies (Ayres and Schneider 2012; Råberg 2014) and which seems meaningful in juvenile trout suffering a potentially lethal disease.

We detected phenotypic correlations between all disease traits (with one exception in the Altja), whereby evolutionary constraints by negative correlations of health were not detected. Interestingly, the correlations increased with pathogen load only in the warmer river. Much of this observation appeared to have been caused by the steeper body-condition decrease with pathogen-load increase in the warmer river. Thus, phenotypic disease trait correlations can, as much as variances, depend on the environment in which they are assessed. This observation also implies that selection for any of the three quantified traits may coselect more strongly for the other traits under worse environmental conditions. In order to more completely reveal the evolutionary implications of environmentally unstable genetic correlations, future investigations with larger sample sizes may study genetic between-traits correlations across environmental conditions.

Confounding Effects between Rivers

Our field study provides rare data on natural variation in resistance and health damage, valuable to evolutionary and ecological immunological research (Baucom and de Roode 2011; Martin et al. 2011; Vander Wal et al. 2014). Field data, however, often incur inferential limitations due to possible confounding effects (Hedrick 1976; Kruuk et al. 2008; Baucom and de Roode 2011; Graham et al. 2011; Bishop et al. 2012; Doeschl-Wilson et al. 2012). We can exclude the possibility that sampling bias (e.g., field sampling order, pedigree structures and qualities) and many technical biases (laboratory processing order, qPCR plate and well effects) underlie the detected between-rivers differences in infection and disease parameters. However, although we focused on water temperature, which is the previously identified major environmental determinant for PKD severity, many unknown factors may have contributed to the differences between rivers (see Hedrick 1976 for many examples). For diseases, many environmental effects can affect health trajectories (Bishop et al. 2012; Doeschl-Wilson et al. 2012). In particular, the water-temperature differences between rivers may have caused different infection onsets; the release of fish-infecting actinospores by bryozoans is seasonally and thermally driven (Tops et al. 2006). The release of actinospores requires temperatures above 14°C (Clifton-Hadley et al. 1986), which were present from May to June during the study year in both rivers. Water-temperature differences between rivers commenced in mid-June, making it therefore likely that infection onset was synchronized between rivers. In addition, the suspected infection-onset period occurred much later than first feeding (in early spring), making it unlikely that the detected genetic resistance or health effects within rivers reflect common environmental effects (Kruuk and Hadfield 2007). Nevertheless, disease pathogenesis may still have differed temporally between rivers if it depended on temperature, such that similar parameter estimates would be possible between rivers with a time lag. However, experimental work on synchronously infected fish, subsequently kept at five different water temperatures (12°–19°C), demonstrated that water temperature between 14° and 19°C did correlate positively with mortality rates but affected neither parasite propagation rate nor temporal kidney pathogenesis, which appeared to depend solely on parasite load (Bettge et al. 2009). Finally, the two rivers could harbor two fish-host populations that differ genetically. However, both reconstructed parental and observed offspring genotypes grouped into genetic clusters across rather than within the neighboring rivers (with little support beyond one common cluster based on offspring genotypes); neutral genetic differentiation appeared very low between rivers ("Assessment of Population Structure" in the appendix) and is generally low along the entire coast (Gross et al. 2013). Thus, it appears more likely that the observed between-rivers differences in resistance and disease severity proceed from the large differences in water temperature.

Sample Size Requirements to Detect Genetic Tolerance Variance

According to previous (Kause 2011) and our own ("Genetic Tolerance Simulations" in the appendix) simulations, reli-

able detection of within-population genetic tolerance variance appears to require tens of thousands of relatives, regardless of whether one uses a family or an animal mixed model based on either full-sib or full-sib half-sib data. These findings may guide design for meaningful future studies of genetic tolerance variance in natural populations. The large sample-size requirement may also explain why genetic tolerance variance has rarely been detected in either cross-sectional or even large-scale longitudinal analyses of natural populations (Lefèvre et al. 2011; Hayward et al. 2014*a*, 2014*b*), although we are unaware of the required sample sizes for longitudinal data (see van de Pol 2012 for requirements to estimate "general" variance but not genetic variance). Interpretations that genetic tolerance may have evolved to a within-population maximum (e.g., Lefèvre et al. 2011) should be viewed with caution if the sample sizes provided low power. Nonetheless, genetic tolerance variance has been detected among natural animal populations (Sternberg et al. 2013) and among inbred, recombinant inbred, or clonal laboratory animal strains (e.g., Råberg et al. 2007; Ayres and Schneider 2009; Howick and Lazzaro 2014). This contrast may occur for several reasons. For example, inbred laboratory strains exhibit little within-strain variation, and differences among them may reflect differences in, for example, accumulated deleterious alleles resulting from inbreeding (Charlesworth and Charlesworth 1987); they are unlikely to reflect variation for natural systems (see also Kruuk et al. 2008). Furthermore, tolerance variance detected on the basis of between-populations variation (estimated as the means) or between-individuals variation within populations (estimated as variance) may not be comparable (Morrissey and Liefting 2016).

Assessing Nonconstant Genetic Variance across Pathogen Load

Animal disease tolerance is usually quantified as a slope of health across pathogen load (Råberg et al. 2007). This concept is sound for the overall response to pathogen load as long as it is linear. However, Louie et al. (2016) recently suggested that the response should be regarded more generally as a curve and stressed that an understanding of distinct portions of a curve may provide a better understanding of resistance-tolerance evolution and effective therapies. Our results, although nonsignificant, support the idea that the genetic variance present for hematocrit may depend on different genes across pathogen load. This idea also emerges if one considers that the genetic correlation between traits may change across pathogen load; a change in the genetic correlation is assumed to depend on a change in underlying genes. Similar ideas were proposed by Kause et al. (2012), who suggested that the genetic architecture of body mass changed with heart-disease severity in chickens. Therefore, regarding tolerance as a set of functions, rather than as a simple slope, may enable a more flexible statistical framework. We suggest moving toward the quantitative genetics framework suggested by Kause and Ødegård (2012), implemented by Kause et al. (2012) for chicken production traits, and here extended to a multivariate setting in a natural animal population. Specifically, for nonlinear tolerance, different genetic variance and/or between-traits correlations within and between distinct curve parts, which may characterize either the initial plateau or the steep slope, can indicate that different sets of genes underlie each part. If we hypothesize, for example, that the plateau of a curve characterizes tolerance without host damage, that is, complete tolerance and an absence of immunopathology, and the steep slope damage by the pathogen or immunopathology, we could test this hypothesis by testing for different genetic variance for each part and for a change in the genetic between-traits correlation across pathogen load between specific parts (i.e., testing whether complete tolerance and incomplete tolerance or immunopathology proceed from different sets of genes). To allow for this flexibility, not much more is needed than to regard intercepts and slopes as one of many possibilities to model nonconstant variance across a continuous variable (de Jong 1995; Meyer and Hill 1997; Morrissey 2014), instead of regarding an intercept as "vigor" and a slope as "tolerance." A comprehensive review of the general ideas and worked examples can be found in Stinchcombe et al. (2012).

Summary

Health after pathogen contact clearly depends on both environmental and genetic effects in the studied host-parasite system. Even though the pathogen load was equal between the two rivers, the relative contribution of nongenetic and genetic variance differed considerably for resistance but was, however, more similar for health damage across pathogen load. A positive genetic correlation between resistance and body size indicates that the two may coevolve, which may maintain genetically based resistance in the absence of disease-induced selection. Importantly, tolerance showed that health decreased disproportionately with pathogen load, and environmental temperature most likely increased the slope of this relationship for all three correlated disease traits. Consequently, the evolutionary importance of resistance and tolerance is expected to vary with both absolute quantity of pathogens and environmental temperature. In a temporally or spatially variable environment, this relationship is predicted to hamper evolution toward either more resistant or more tolerant hosts.

Acknowledgments

The authors are thankful to A. Nurkse, L. Pukk, and M. Visse for fieldwork help and to K. Salminen for genotyping. We very much thank Y. Michalakis, S. Nuismer, and three anon-

ymous reviewers for their constructive comments that greatly improved earlier versions of the manuscript. This study was supported by an Estonian Ministry of Education and Research Institutional Research Fund (project IUT8-2), an Academy of Finland grant (266321), the Estonian University of Life Sciences Development Fund, and a German Research Foundation Research Fellowship (DE 2405/1–1).

Literature Cited

Abd-Elfattah, A., G. Kumar, H. Soliman, and M. El-Matbouli. 2014. Persistence of *Tetracapsuloides bryosalmonae* (Myxozoa) in chronically infected brown trout *Salmo trutta*. Diseases of Aquatic Organisms 111:41–49.

Adelman, J. S., and D. M. Hawley. 2017. Tolerance of infection: a role for animal behavior, potential immune mechanisms, and consequences for parasite transmission. Hormones and Behavior 88:79–86.

Aljanabi, S. M., and I. Martinez. 1997. Universal and rapid salt-extraction of high quality genomic DNA for PCR-based techniques. Nucleic Acids Research 25:4692–4693.

Anderson, C. L., E. U. Canning, and B. Okamura. 1999. Molecular data implicate bryozoans as hosts for PKX (phylum Myxozoa) and identify a clade of bryozoan parasites within the Myxozoa. Parasitology 119:555–561.

Ayres, J. S., and D. S. Schneider. 2009. The role of anorexia in resistance and tolerance to infections in *Drosophila*. PLoS Biology 7(7): e1000150. doi:10.1371/journal.pbio.1000150.

———. 2012. Tolerance of infections. Annual Review of Immunology 30:271–294.

Baerwald, M. R., J. L. Petersen, R. P. Hedrick, G. J. Schisler, and B. May. 2011. A major effect quantitative trait locus for whirling disease resistance identified in rainbow trout (*Oncorhynchus mykiss*). Heredity 106:920–926.

Barrett, L. G., P. H. Thrall, J. J. Burdon, and C. C. Linde. 2008. Life history determines genetic structure and evolutionary potential of host-parasite interactions. Trends in Ecology and Evolution 23:678–685.

Baucom, R. S., and J. C. de Roode. 2011. Ecological immunology and tolerance in plants and animals. Functional Ecology 25:18–28.

Best, A., A. White, and M. Boots. 2008. Maintenance of host variation in tolerance to pathogens and parasites. Proceedings of the National Academy of Sciences of the USA 105:20786–20791.

Bettge, K., H. Segner, R. Burki, H. Schmidt-Posthaus, and T. Wahli. 2009. Proliferative kidney disease (PKD) of rainbow trout: temperature- and time-related changes of *Tetracapsuloides bryosalmonae* DNA in the kidney. Parasitology 136:615–625.

Bishop, S. C., A. B. Doeschl-Wilson, and J. A. Woolliams. 2012. Uses and implications of field disease data for livestock genomic and genetics studies. Frontiers in Genetics 3:114. doi:10.3389/fgene.2012.00114.

Blanchet, S., O. Rey, and G. Loot. 2010. Evidence for host variation in parasite tolerance in a wild fish population. Evolutionary Ecology 24:1129–1139.

Boots, M., and R. G. Bowers. 1999. Three mechanisms of host resistance to microparasites—avoidance, recovery and tolerance—show different evolutionary dynamics. Journal of Theoretical Biology 201:13–23.

Boots, M., A. White, A. Best, and R. Bowers. 2012. The importance of who infects whom: the evolution of diversity in host resistance to infectious disease. Ecology Letters 15:1104–1111.

Bruneaux, M., M. Visse, R. Gross, L. Pukk, L. Saks, and A. Vasemägi. 2017. Parasite infection and decreased thermal tolerance: impact of proliferative kidney disease on a wild salmonid fish in the context of climate change. Functional Ecology 31:216–226.

Brunner, F. S., and C. Eizaguirre. 2016. Can environmental change affect host/parasite-mediated speciation? Zoology (Jena) 119:384–394.

Bulmer, M. G. 1971. The effect of selection on genetic variability. American Naturalist 105:201–211.

Butler, D. G., B. R. Cullis, A. R. Gilmour, and B. J. Gogel. 2009. Mixed models for S language environments ASReml-R reference manual. Queensland Department of Primary Industries and Fisheries, Brisbane, Australia.

Charlesworth, D., and B. Charlesworth. 1987. Inbreeding depression and its evolutionary consequences. Annual Review of Ecology and Systematics 18:237–268.

Charmantier, A., and D. Garant. 2005. Environmental quality and evolutionary potential: lessons from wild populations. Proceedings of the Royal Society B 272:1415–1425.

Clifton-Hadley, R. S., D. Bucke, and R. H. Richards. 1987. A study of the sequential clinical and pathological-changes during proliferative kidney disease in rainbow trout, *Salmo gairdneri* Richardson. Journal of Fish Diseases 10:335–352.

Clifton-Hadley, R. S., R. H. Richards, and D. Bucke. 1986. Proliferative kidney-disease (PKD) in rainbow trout *Salmo gairdneri*: further observations on the effects of water temperature. Aquaculture 55:165–171.

Coltman, D. W., J. Pilkington, L. E. B. Kruuk, K. Wilson, and J. M. Pemberton. 2001. Positive genetic correlation between parasite resistance and body size in a free-living ungulate population. Evolution 55:2116–2125.

Dash, M., and A. Vasemägi. 2014. Proliferative kidney disease (PKD) agent *Tetracapsuloides bryosalmonae* in brown trout populations in Estonia. Diseases of Aquatic Organisms 109:139–148.

Debes, P. V., R. Gross, and A. Vasemägi. 2017. Data from: Quantitative genetic variation in, and environmental effects on, pathogen resistance and temperature-dependent disease severity in a wild trout. American Naturalist, Dryad Digital Repository, http://dx.doi.org/10.5061/dryad.12758.

de Jong, G. 1995. Phenotypic plasticity as a product of selection in a variable environment. American Naturalist 145:493–512.

Doeschl-Wilson, A. B., S. C. Bishop, I. Kyriazakis, and B. Villanueva. 2012. Novel methods for quantifying individual host response to infectious pathogens for genetic analyses. Frontiers in Genetics 3:266. doi:10.3389/fgene.2012.00266.

Falconer, D. S. 1952. The problem of environment and selection. American Naturalist 86:293–298.

Ferguson, H. W. 1981. The effects of water temperature on the development of proliferative kidney disease in rainbow trout, *Salmo gairdneri* Richardson. Journal of Fish Diseases 4:175–177.

Fineblum, W. L., and M. D. Rausher. 1995. Tradeoff between resistance and tolerance to herbivore damage in a morning glory. Nature 377:517–520.

Fischer, T. M., A. R. Gilmour, and J. H. van der Werf. 2004. Computing approximate standard errors for genetic parameters derived from random regression models fitted by average information REML. Genetics, Selection, Evolution 36:363–369.

Gay, M., B. Okamura, and P. de Kinkelin. 2001. Evidence that infectious stages of *Tetracapsula bryosalmonae* for rainbow trout *Oncorhynchus mykiss* are present throughout the year. Diseases of Aquatic Organisms 46:31–40.

Gjedrem, T. 2005. Selection and breeding programs in aquaculture. Springer, Dordrecht, Netherlands.

Grabner, D. S., and M. El-Matbouli. 2009. Comparison of the susceptibility of brown trout (*Salmo trutta*) and four rainbow trout (*Oncorhynchus mykiss*) strains to the myxozoan *Tetracapsuloides bryosalmonae*, the causative agent of proliferative kidney disease (PKD). Veterinary Parasitology 165:200–206.

Graham, A. L., D. M. Shuker, L. C. Pollitt, S. K. J. R. Auld, A. J. Wilson, and T. J. Little. 2011. Fitness consequences of immune responses: strengthening the empirical framework for ecoimmunology. Functional Ecology 25:5–17.

Gross, R., M.-L. Koljonen, J. Koskiniemi, and O. Burimski. 2013. Genetic studies of sea trout (report of the results of Work Package 2). Healthy fish stocks—indicators of successful river basin management (HEALFISH). Central Baltic INTERREG IV A programme, Tartu and Helsinki. https://www.ely-keskus.fi/documents/8849951/16465766/Gross+et+al+2013+Genetic+studies+of+sea+trout+%28report+of+the+results+of+HEALFISH+Work+Package+2%29.pdf/bcd7bad0-86f6-4b3d-b2fa-3029fc421132.

Hadfield, J. D. 2008. Estimating evolutionary parameters when viability selection is operating. Proceedings of the Royal Society B 275:723–734.

Hayward, A. D., R. Garnier, K. A. Watt, J. G. Pilkington, B. T. Grenfell, J. B. Matthews, J. M. Pemberton, D. H. Nussey, and A. L. Graham. 2014*a*. Heritable, heterogeneous, and costly resistance of sheep against nematodes and potential feedbacks to epidemiological dynamics. American Naturalist 184(suppl.):S58–S76.

Hayward, A. D., D. H. Nussey, A. J. Wilson, C. Berenos, J. G. Pilkington, K. A. Watt, J. M. Pemberton, and A. L. Graham. 2014*b*. Natural selection on individual variation in tolerance of gastrointestinal nematode infection. PLoS Biology 12(7):e1001917. doi:10.1371/journal.pbio.1001917.

Hedrick, P. W. 1976. Genetic polymorphism in heterogeneous environments. Annual Review of Ecology, Evolution, and Systematics 7:1–32.

Hedrick, R. P., E. MacConnell, and P. de Kinkelin. 1993. Proliferative kidney disease of salmonid fish. Annual Review of Fish Diseases 3:277–290.

Henderson, C. R. 1973. Sire evaluation and genetic trends. Journal of Animal Science 1973(Symposium):10–41.

Hill, S. L., and B. Okamura. 2007. Endoparasitism in colonial hosts: patterns and processes. Parasitology 134:841–852.

Hoffmann, A. A., and J. Merilä. 1999. Heritable variation and evolution under favourable and unfavourable conditions. Trends in Ecology and Evolution 14:96–101.

Horn, T., B. C. Robertson, and N. J. Gemmell. 2010. The use of telomere length in ecology and evolutionary biology. Heredity 105:497–506.

Houle, D. 1991. Genetic covariance of fitness correlates: what genetic correlations are made of and why it matters. Evolution 45:630–648.

Howick, V. M., and B. P. Lazzaro. 2014. Genotype and diet shape resistance and tolerance across distinct phases of bacterial infection. BMC Evolutionary Biology 14:56. doi:10.1186/1471-2148-14-56.

Johnson, P. C., and D. T. Haydon. 2007. Maximum-likelihood estimation of allelic dropout and false allele error rates from microsatellite genotypes in the absence of reference data. Genetics 175:827–842.

Jones, O. R., and J. Wang. 2010. COLONY: a program for parentage and sibship inference from multilocus genotype data. Molecular Ecology Resources 10:551–555.

Kause, A. 2011. Genetic analysis of tolerance to infections using random regressions: a simulation study. Genetical Research 93:291–302.

Kause, A., and J. Ødegård. 2012. The genetic analysis of tolerance to infections: a review. Frontiers in Genetics 3:262. doi:10.3389/fgene.2012.00262.

Kause, A., S. van Dalen, and H. Bovenhuis. 2012. Genetics of ascites resistance and tolerance in chicken: a random regression approach. G3: Genes, Genomes, Genetics 2:527–535.

Kenward, M. G., and J. H. Roger. 1997. Small sample inference for fixed effects from restricted maximum likelihood. Biometrics 53:983–997.

Kruuk, L. E. B. 2004. Estimating genetic parameters in natural populations using the "animal model." Philosophical Transactions of the Royal Society B 359:873–890.

Kruuk, L. E. B., and J. D. Hadfield. 2007. How to separate genetic and environmental causes of similarity between relatives. Journal of Evolutionary Biology 20:1890–1903.

Kruuk, L. E. B., J. Merilä, and B. C. Sheldon. 2003. When environmental variation short-circuits natural selection. Trends in Ecology and Evolution 18:207–209.

Kruuk, L. E. B., J. Slate, and A. J. Wilson. 2008. New answers for old questions: the evolutionary quantitative genetics of wild animal populations. Annual Review of Ecology, Evolution, and Systematics 39:525–548.

Kumar, G., A. Abd-Elfattah, M. Saleh, and M. El-Matbouli. 2013. Fate of *Tetracapsuloides bryosalmonae* (Myxozoa) after infection of brown trout *Salmo trutta* and rainbow trout *Oncorhynchus mykiss*. Diseases of Aquatic Organisms 107:9–18.

Lazzaro, B. P., and T. J. Little. 2009. Immunity in a variable world. Philosophical Transactions of the Royal Society B 364:15–26.

Lefèvre, T., A. J. Williams, and J. C. de Roode. 2011. Genetic variation in resistance, but not tolerance, to a protozoan parasite in the monarch butterfly. Proceedings of the Royal Society B 278:751–759.

Lillehammer, M., J. Ødegård, and T. H. Meuwissen. 2009. Reducing the bias of estimates of genotype by environment interactions in random regression sire models. Genetics, Selection, Evolution 41:30. doi:10.1186/1297-9686-41-30.

Lively, C. M., J. C. de Roode, M. A. Duffy, A. L. Graham, and B. Koskella. 2014. Interesting open questions in disease ecology and evolution. American Naturalist 184(suppl.):S1–S8.

Longshaw, M., R.-M. Le Deuff, A. F. Harris, and S. W. Feist. 2002. Development of proliferative kidney disease in rainbow trout, *Oncorhynchus mykiss* (Walbaum), following short-term exposure to *Tetracapsula bryosalmonae* infected bryozoans. Journal of Fish Diseases 25:443–449.

Louie, A., K. H. Song, A. Hotson, A. Thomas Tate, and D. S. Schneider. 2016. How many parameters does it take to describe disease tolerance? PLoS Biology 14(4):e1002435. doi:10.1371/journal.pbio.1002435.

Mackinnon, M. J., and A. F. Read. 1999. Genetic relationships between parasite virulence and transmission in the rodent malaria *Plasmodium chabaudi*. Evolution 53:689–703.

Martin, L. B., D. M. Hawley, and D. R. Ardia. 2011. An introduction to ecological immunology. Functional Ecology 25:1–4.

Mazé-Guilmo, E., G. Loot, D. J. Páez, T. Lefèvre, and S. Blanchet. 2014. Heritable variation in host tolerance and resistance inferred from a wild host-parasite system. Proceedings of the Royal Society B 281:20132567. doi:10.1098/rspb.2013.2567.

Medzhitov, R., D. S. Schneider, and M. P. Soares. 2012. Disease tolerance as a defense strategy. Science 335:936–941.

Meyer, K., and W. G. Hill. 1997. Estimation of genetic and phenotypic covariance functions for longitudinal or 'repeated' records by restricted maximum likelihood. Livestock Production Science 47:185–200.

Miller, M. P., and E. R. Vincent. 2008. Rapid natural selection for resistance to an introduced parasite of rainbow trout. Evolutionary Applications 1:336–341.

Miller, M. R., A. White, and M. Boots. 2005. The evolution of host resistance: tolerance and control as distinct strategies. Journal of Theoretical Biology 236:198–207.

Morris, D. J., and A. Adams. 2006. Transmission of *Tetracapsuloides bryosalmonae* (Myxozoa: Malacosporea), the causative organism of salmonid proliferative kidney disease, to the freshwater bryozoan *Fredericella sultana*. Parasitology 133:701–709.

Morrissey, M. B. 2014. Selection and evolution of causally covarying traits. Evolution 68:1748–1761.

Morrissey, M. B., L. E. B. Kruuk, and A. J. Wilson. 2010. The danger of applying the breeder's equation in observational studies of natural populations. Journal of Evolutionary Biology 23:2277–2288.

Morrissey, M. B., and M. Liefting. 2016. Variation in reaction norms: statistical considerations and biological interpretation. Evolution 70: 1944–1959.

Mostowy, R., and J. Engelstadter. 2011. The impact of environmental change on host-parasite coevolutionary dynamics. Proceedings of the Royal Society B 278:2283–2292.

Nault, B. A., and G. G. Kennedy. 1993. Limitations of using regression and mean separation analyses for describing the response of crop yield to defoliation: a case study of the Colorado potato beetle (Coleoptera: Chrysomelidae) on potato. Journal of Economic Entomology 91:7–19.

Neudecker, R. A., T. E. McMahon, and E. R. Vincent. 2012. Spatial and temporal variation of whirling disease risk in Montana spring creeks and rivers. Journal of Aquatic Animal Health 24:201–212.

Okamura, B., H. Hartikainen, H. Schmidt-Posthaus, and T. Wahli. 2011. Life cycle complexity, environmental change and the emerging status of salmonid proliferative kidney disease. Freshwater Biology 56:735–753.

Pfaffl, M. W. 2001. A new mathematical model for relative quantification in real-time RT-PCR. Nucleic Acids Research 29:e45.

Råberg, L. 2014. How to live with the enemy: understanding tolerance to parasites. PLoS Biology 12(11):e1001989. doi:10.1371/journal.pbio.1001989.

Råberg, L., A. L. Graham, and A. F. Read. 2009. Decomposing health: tolerance and resistance to parasites in animals. Philosophical Transactions of the Royal Society B 364:37–49.

Råberg, L., D. Sim, and A. F. Read. 2007. Disentangling genetic variation for resistance and tolerance to infectious diseases in animals. Science 318:812–814.

Rausher, M. D. 1992. The measurement of selection on quantitative traits: biases due to environmental covariances between traits and fitness. Evolution 46:616–626.

Restif, O., and J. C. Koella. 2004. Concurrent evolution of resistance and tolerance to pathogens. American Naturalist 164:E90–E102.

Rosenthal, J. P., and P. M. Kotanen. 1994. Terrestrial plant tolerance to herbivory. Trends in Ecology and Evolution 9:145–148.

Roy, B. A., and J. W. Kirchner. 2000. Evolutionary dynamics of pathogen resistance and tolerance. Evolution 54:51–63.

Sarker, S., D. M. Kallert, R. P. Hedrick, and M. El-Matbouli. 2015. Whirling disease revisited: pathogenesis, parasite biology and disease intervention. Diseases of Aquatic Organisms 114:155–175.

Schaeffer, L. R. 2004. Application of random regression models in animal breeding. Livestock Production Science 86:35–45.

Schmidt-Posthaus, H., K. Bettge, U. Forster, H. Segner, and T. Wahli. 2012. Kidney pathology and parasite intensity in rainbow trout *Oncorhynchus mykiss* surviving proliferative kidney disease: time course and influence of temperature. Diseases of Aquatic Organisms 97: 207–218.

Schneider, C. A., W. S. Rasband, and K. W. Eliceiri. 2012. NIH Image to ImageJ: 25 years of image analysis. Nature Methods 9:671–675.

Scholthof, K.-B. G. 2007. The disease triangle: pathogens, the environment and society. Nature Reviews Microbiology 5:152–156.

Seppälä, O. 2015. Natural selection on quantitative immune defence traits: a comparison between theory and data. Journal of Evolutionary Biology 28:1–9.

Sheldon, B. C., and S. Verhulst. 1996. Ecological immunology: costly parasite defences and trade-offs in evolutionary ecology. Trends in Ecology and Evolution 11:317–321.

Simms, E. L., and M. D. Rausher. 1987. Costs and benefits of plant-resistance to herbivory. American Naturalist 130:570–581.

Sogard, S. M. 1997. Size-selective mortality in the juvenile stage of teleost fishes: a review. Bulletin of Marine Science 60:1129–1157.

Sternberg, E. D., H. Li, R. Wang, C. Gowler, and J. C. de Roode. 2013. Patterns of host-parasite adaptation in three populations of monarch butterflies infected with a naturally occurring protozoan disease: virulence, resistance, and tolerance. American Naturalist 182: E235–E248.

Sterud, E., T. Forseth, O. Ugedal, T. T. Poppe, A. Jørgensen, T. Bruheim, H.-P. Fjeldstad, and T. A. Mo. 2007. Severe mortality in wild Atlantic salmon *Salmo salar* due to proliferative kidney disease (PKD) caused by *Tetracapsuloides bryosalmonae* (Myxozoa). Diseases of Aquatic Organisms 77:191–198.

Stinchcombe, J. R., Function-Valued Traits Working Group, and M. Kirkpatrick. 2012. Genetics and evolution of function-valued traits: understanding environmentally responsive phenotypes. Trends in Ecology and Evolution 27:637–647.

Stowe, K. A., R. J. Marquis, C. G. Hochwender, and E. L. Simms. 2000. The evolutionary ecology of tolerance to consumer damage. Annual Review of Ecology and Systematics 31:565–595.

Tenesa, A., and C. S. Haley. 2013. The heritability of human disease: estimation, uses and abuses. Nature Reviews Genetics 14:139–149.

Tops, S., W. Lockwood, and B. Okamura. 2006. Temperature-driven proliferation of *Tetracapsuloides bryosalmonae* in bryozoan hosts portends salmonid declines. Diseases of Aquatic Organisms 70:227–236.

Vale, P. F., and T. J. Little. 2012. Fecundity compensation and tolerance to a sterilizing pathogen in *Daphnia*. Journal of Evolutionary Biology 25:1888–1896.

van de Pol, M. 2012. Quantifying individual variation in reaction norms: how study design affects the accuracy, precision and power of random regression models. Methods in Ecology and Evolution 3:268–280.

van der Most, P. J., B. de Jong, H. K. Parmentier, and S. Verhulst. 2011. Trade-off between growth and immune function: a meta-analysis of selection experiments. Functional Ecology 25:74–80.

Vander Wal, E., D. Garant, S. Calmé, C. A. Chapman, M. Festa-Bianchet, V. Millien, S. Rioux-Paquette, and F. Pelletier. 2014. Applying evolutionary concepts to wildlife disease ecology and management. Evolutionary Applications 7:856–868.

Walker, J. C. 1965. Use of environmental factors in screening for disease resistance. Annual Review of Phytopathology 3:197–208.

Weis, A. E., E. L. Simms, and M. E. Hochberg. 2000. Will plant vigor and tolerance be genetically correlated? effects of intrinsic growth rate and self-limitation on re-growth. Evolutionary Ecology 14: 331–352.

Wilson, A. J., J. M. Pemberton, J. G. Pilkington, D. W. Coltman, D. V. Mifsud, T. H. Clutton-Brock, and L. E. B. Kruuk. 2006. Environ-

mental coupling of selection and heritability limits evolution. PLoS Biology 4(7):e216. doi:10.1371/journal.pbio.0040216.

Wilson, A. J., D. Réale, M. N. Clements, M. M. Morrissey, E. Postma, C. A. Walling, L. E. B. Kruuk, and D. H. Nussey. 2010. An ecologist's guide to the animal model. Journal of Animal Ecology 79:13–26.

Wolinska, J., and K. C. King. 2009. Environment can alter selection in host-parasite interactions. Trends in Parasitology 25:236–244.

Associate Editor: Scott L. Nuismer
Editor: Yannis Michalakis

The colder river Altja (*left*) and the warmer river Mustoja (*right*) from where the studied Estonian brown trout (*Salmo trutta*) individuals were sampled. Photo credits: Anti Vasemägi, Paul Debes, 2014.